MEASUREMENT OF TOTAL EMISSIVITY OF SURFACES AT LOW TEMPERATURES

A THESIS

Presented to

the Faculty of the Graduate Division

Georgia Institute of Technology

In Partial Fulfillment

of the Requirements for the Degree

Master of Science in Chemical Engineering

By

Harry Cheung

June 1955

"In presenting the dissertation as a partial fulfillment of the requirements for an advanced degree from the Georgia Institute of Technology, I agree that the Library of the Institution shall make it available for inspection and circulation in accordance with its regulations governing materials of this type. I agree that permission to copy from, or to publish from, this dissertation may be granted by the professor under whose direction it was written, or such copying or publication is solely for scholarly purposes and does not involve potential financial gain. It is understood that any copying from, or publication of, this dissertation which involves potential financial gain will not be allowed without written permission.

_____"

MEASUREMENT OF TOTAL EMISSIVITY OF

SURFACES AT LOW TEMPERATURES

Approved

Thesis Advisor

Date Approved by Chairman June 1, 1971

ACKNOWLEDGEMENTS

On the completion of this work, I wish to express my sincerest thanks to Dr. W. T. Ziegler, not only for his suggestion of this problem, but also for his most valuable aid and guidance in its prosecution. I wish to thank Dr. H. C. Lewis and Dr. W. B. Harrison for their suggestions. I am indebted to Mr. George Ragovis for his many Russian translations.

I also wish to express my gratitude for the laboratory facilities furnished by the Engineering Experiment Station, Georgia Institute of Technology.

CONTENTS

ABSTRACT

Measurement of Total Emissivity of Surfaces
at Low Temperatures
(108)

The object of this work is to provide additional information for the design of vacuum vessels for the storage and conveyance of liquefied gases and to provide information for the estimation of thermal radiation transfer in low temperature apparatus. This information is presented in the form of apparent emissivities.

Much of the presently available data or emissivity has only limited applicability because optimum quality surfaces were studied. For this reason the present study was planned to provide data not on the "best" surfaces, but on surfaces cleaned, polished, or otherwise prepared in ways that can be copied in practice. The cryostat used for radiation studies was designed in such a manner that the radiation transfer could be determined with minimum corrections for other heat leaks. The heat transfer was determined by metering the evaporated gas leaving the cryostat.

The results of the surfaces studied at liquid nitrogen temperature are tabulated in Table I.

TABLE I

Summary of Results

Hot Surface (273°K)	Cold Surface (77.4°K)	Emissivity
Lampblack*	Lampblack*	0.87
	Scotch Tape	0.89
	G. E. Adhesive No. 7031	0.88
	Bakelite Lacquer	0.87
	Brass	0.098
	Monel	0.11
	Aluminum Foil	0.043
	Brass (tarnished)	0.11
	Wood's Metal	0.16
	Chromium	0.084
	Apiezon N	0.17
	40 Sn/60 Pb Solder	0.047

All nonmetallic surfaces were found to have high emissivities. As a general rule, most metallic surfaces have low emissivities. Aluminum foil, loosely wrapped, is an excellent reflector. This material is recommended for the shielding of high emissivity surfaces. It is easy to handle and is very economical.

Brass, monel metal, chromium, and aluminum foil, have previously been investigated by other researchers. The remaining surfaces in Table I have not been investigated specifically prior to this research.

---

*A suspension of lampblack in Glyptal, a varnish (No. 1202) made by the General Electric Company.

LIST OF TABLES

LIST OF FIGURES

CHAPTER I

INTRODUCTION

To the cryogenic engineer or scientist the problem of reducing the heat transmission from the surroundings to the produced liquefied gas is a never ending problem. It is hoped that this thesis will be a small contribution to this never ending problem.

The object of this work is to provide additional information for the design of vacuum vessels for the storage and conveyance of liquefied gases and to provide information for the estimation of thermal radiation transfer in low temperature apparatus. This information will be presented in the form of apparent emissivities. The surfaces investigated in this research are yellow brass, monel metal, aluminum foil, oxidized brass, plated chromium, Wood's metal, 40/60 solder, lampblack[1], Scotch tape, bakelite, adhesive[2], and Apiezon N[3]. These surfaces were investigated because they are often encountered in low temperature work.

---

[1]A suspension of lampblack in Glyptal, a varnish made by the General Electric Company.

[2]General Electric adhesive No. 7031.

[3]Apiezon N, a vacuum grease manufactured by the Metropolitan-Vickers Electrical Company Ltd.

Brass and monel metal were investigated because they are often used in the construction of low temperature apparatus. Oxidized brass was investigated because brass will oxidize over a relatively short period of time. The observation of the change in emissivity will be helpful in design. Chromium was investigated because of the ease of plating films of this material on many metallic surfaces. Loosely wrapped aluminum foil is of interest since this would be a very simple and inexpensive method of decreasing the radiation transfer. Wood's metal has the property of a low melting point. Because of this property, it is often used in regions that can tolerate little temperature rise in soldering. Solder having the composition forty per cent tin and sixty per cent lead by weight is a solder commonly used in low temperature equipment. The emissivities of these two solders are of interest because parts of the apparatus are often covered with these substances. The nonmetals except for Apiezon N are used in electrical insulation and in attaching wires to surfaces. A thin film of Apiezon N is transparent and does not affect the polished surface of a metal. By applying such a thin film to a polished metal, one is able to observe the effect of emissivity change upon a polished surface due to the presence of an unseen organic compound.

The most notable device in low temperature heat

reduction is the vacuum vessel. The vacuum vessel was introduced by Sir James Dewar. Since this classical work, there has been a considerable number of researches on vacuum-jacketed vessels; but even now the subject does not seem to have been studied as completely as its practical importance and theoretical interest would seem to justify. In the following paragraphs, a brief review of the literature will be presented. All types of "heat leaks" to Dewar vessels will be included in this review.

A brief review of the literature indicates the following publications on the subject. In 1893 Dewar (1)[4] published his work on the vacuum vessel, although he had used a highly-exhausted vessel in calorimetric experiments as early as 1873. By evacuating a double wall vessel Dewar found that the evaporation rate of oxygen and ethylene was decreased by a factor of 5. When the walls of the vessel were silvered, the evaporation rate of the same two substances decreased by a factor of 10. In 1893 he published a study of the efficiencies of glass vacuum flasks with various coatings on the surface and with various substances in the vacuum space. He only got approximate results (2). Although Dewar and Tait had used charcoal to produce a vacuum in 1874, it was not until 1904 that Dewar drew attention to the use of charcoal cooled in liquid air to

---

[4]Numbers in parentheses refer to items in the Bibliography.

give high vacua (3). This enabled him to develop the metal vacuum vessel.

After the preliminary work by Dewar, various researchers investigated the physics of the vacuum vessel. Seven causes of heat flow to the inner vessel of a vacuum container were found. These seven causes of heat flow were listed in a report by the Oxygen Research Committee of the Department of Scientific and Industrial Research (London) (4).

(1) Conduction through the residual gas in the vacuum space.

(2) Convection through the residual gas in the vacuum space.

(3) Radiation across the vacuum space.

(4) Conduction along the neck of the flask.

(5) Radiation through the neck aperture.

(6) Conduction through supporting materials, if any, across the vacuum space.

(7) Convection in the interior space of the flask and neck.

Of these seven heat flows, four of them predominate (5):

(1) Conduction along the neck of the flask.

(2) Conduction through the residual gas in the vacuum space.

(3) Radiation through the neck aperture.

(4) Radiation across the vacuum space.

Each of the above factors has been considered in the design

of the apparatus used in this research. A discussion of these considerations can be found in Chapter 4.

Conduction Along the Neck of the Flask.--Banneitz, Rhein, and Kurge (6), devised a method for measuring the conduction along the neck independent of other losses. Briggs (7), using the method of Banneitz et al., found that the evaporation due to neck conduction decreased as the evaporation rate is increased because of the heat transfer of the cold evaporated gas traveling up the neck. The method was to place another tube in the neck of the vessel, thereby increasing the area of conduction. By observing the increase in evaporation the neck loss could be determined.

Hoag (8) and Meissner (9) made calculations for the estimation of the evaporation increase due to conduction along the neck. Hoag assumed the complete transfer of heat from the neck to the cold evaporated gas. Meissner assumed the temperature change along the neck to be a linear function of length. Ryabinin (5) made various experiments verifying the method of Hoag. His experimental method consisted of a high thermal conductivity ring with a thermocouple enclosed by a low thermal conductivity material on three sides. By sliding the ring up and down the neck of a Dewar flask he could obtain the temperature distribution of the wall or of the gas depending upon which side the high thermal conductivity material was inserted.

In more recent years, Sydoriak and Sommers (10), and Henry (11), have made similar calculations for helium vessels. Both used the same line of thought as Hoag. Sydoriak and Sommers assumed that any level in the Dewar vessel the temperatures of the vapor and of the adjacent wall are the same. Henry applies a finite difference treatment of the problem, making assumptions similar to that of Sydoriak and Sommers.

Perhaps the most unique method for the determination of neck "heat leak" was devised by Wexler (12). Wexler inserts a heater into the Dewar flask. At high heat inputs the evaporation rate became a linear function of heat input. By extrapolating this linear relationship to zero input one can determine the heat leak produced by the neck, which is the difference of the observed and the extrapolated value.

Conduction Through the Residual Gas in the Vacuum Space.-- Soddy and Berry (13) by the use of 5 gases showed experimentally that the heat transmitting power of the gas varies directly as the pressure at pressures up to a few millionths of an atmosphere. The relation observed expressed in mathematical form is

$$Q = C\ (T_2 - T_1)\ A\ P \qquad (1)$$

Where C - Factor for a Specific Gas

T - Temperature (T_2 - Hot, T_1 - Cold)

A - Area

P - Pressure

Q - Heat Transmitted

The above relation is approximately equal to a modified form of the Knudsen equation due to Ryabinin (5) which states

$$Q = N\sqrt{\frac{273}{T}}\,(T_2 - T_1)\,A\,P \qquad (2)$$

in which N is a factor for a specific gas and T is the temperature of the rarified gas, assumed equal to the arithmetic mean of T_1 and T_2. Knudsen (14) derived the relation

$$E_t = \sqrt{\frac{2}{\pi}}\,P\,\frac{1}{\sqrt{\rho}}\,\frac{T_1 - T_2}{\sqrt{273\,T}} \qquad (3)$$

from the kinetic theory of gases. E_t is the energy gained per unit area of receiving surface. ρ is the specific gravity of the gas at a temperature of 273°K and a pressure of one dyne per square centimeter. T is the temperature of the rarified gas with T_1 and T_2 being the hot and cold surface temperatures, respectively. When the temperature of the rarified gas is constant, the energy transmitted is a linear function of the pressure.

Radiation Through the Neck Aperture.--It is general practice to assume the radiation through the neck aperture to be black body radiation, which can be calculated by the Stefan-Boltzmann Law.

Radiation Across the Vacuum Space.--Blackman (2) devised an apparatus for the measurement of the heat transmission by radiation across the vacuum space independent of all the

other heat losses by the addition of a heat transfer reservoir to prevent conduction down the neck. If the neck is small and the vacuum very high, the radiation across the vacuum space is approximately equal to all the "heat leak". By metering the evaporation rate, Blackman was able to calculate the apparent emissivity of the surface studied. Before Blackman's work, all the other researchers have evaluated the various heat losses and subtracted from the total heat loss to obtain the radiation loss across the vacuum space. Blackman points out that surface conditions such as cold working, cleanness, etc. are important factors governing radiation transfer.

It usually has been taken for granted, following Dewar, that the vacuum adjacent surfaces in metal vessels should be as highly polished as possible; but this is not necessarily so, because a highly polished surface is generally covered with a thin oxide film and also retains some of the polishing material. Judgment of the surface by eye may in some cases lead to erroneous results. The visible region of wave lengths detectable by the eye is approximately from 0.4 to 0.7 microns but the maximum energy is at 9.7 microns approximately for blackbody radiation at room temperature as indicated by Wien's Displacement Law. This fact will be developed further in the next Chapter in the discussion of theoretical concepts.

Perhaps the most complete summary of apparent emissivities for low temperatures has been published by

Fulk, Reynolds, and Park (15). This research was fortunate in obtaining a copy of NBS-AEC Cryogenic Engineering Laboratory Note 54-9 from M. M. Fulk. The Laboratory Note 54-9 was a preliminary summary of low temperature emissivities for the new Handbook of Physics, edited by M. Zemansky. Fulk, Reynolds, and Park have used various types of apparatus for measuring low temperature emissivity. They have used a metallic reservoir type, a plastic type, and a glass type apparatus in their work.

Other Types of Vacuum Vessels.--The triple-walled vessel and the double-double walled vessel will be mentioned. The triple-walled vessel is a vacuum vessel with a radiation shield of some type inserted in the vacuum space between the outer and inner walls with minimum contact to these walls. Roebuck (16) designed and built a 120 liter vessel of the triple-walled type for the storage of liquid air. It was found that the vessel agreed very well with theory (17), which indicated that the radiation loss should be approximately one-half of that of the double-walled vessel. Rips (18) calculated that the radiation loss should be decreased by 40 per cent and the evaporation rate be decreased by 25 per cent for a silvered spherical Dewar vessel of 15 liter capacity as a container for liquid oxygen.

The double-double walled vacuum vessel is actually one vacuum vessel in another. Vessels of this type are used for the storage of hydrogen and helium with liquid air or nitrogen in the outer vacuum vessel. Giauque (19),

Henry and Dolecek (20), and Wexler (12) have done work along these lines.

The use of vacuum-powder insulation will be also mentioned. Katan (21) covers this subject up to 1951. He indicates that powders under vacuum are good low temperature insulators.

At present, a considerable amount of work is being done in the field of low temperature radiation. Some of the researchers, other than ourselves, are M. M. Fulk of the National Bureau of Standards at Boulder, Colorado, and F. J. Zimmerman (22) at the Arthur D. Little Company, Cambridge, Massachusetts.

CHAPTER II[5]

THEORY

List of Symbols.--The notation and terminology used in this thesis are similar to those of McAdams (23).

A	Area of a surface; A_1, 2, 3, area of a source-sink-type surface (cm^2)
c_1, c_2	Dimensional constants in Planck equation
F	Configuration factor also called view factor and geometric factor
$\mathcal{F}$	Over-all interchange factor, a function of e and F
P	Pressure (mm Hg)
P_B	Barometric pressure (mm Hg)
P_w	Partial pressure of water (mm Hg)
T	Temperature (^oK)
Q	Heat transferred (cal/min)
t	Time (min)
R_r	Flowrate of sample container when full (cc/min)
W	Total emissive power of source
W_B	Total emissive power of black source
λ	Wave length
H_v	Heat of vaporization
W_λ	Monochromatic emissive power of source

---

[5]Much of the material covered in this Chapter can be found in the books by Richtmyer and Kennard (24) and McAdams (23).

W_{B_λ}	Monochromatic emissive power of black source
α	Absorptivity
e	Emissivity equal to $\frac{W}{W_B}$
1, 2, 3,	Subscripts indicate the source receiving and radiating energy

General Introduction to Radiation Theory.--It is a matter of common observation that bodies when heated emit radiant energy--or, more simply, thermal radiation--the quantity and quality of which depends, for any given body, on the temperature of that body. It is a characteristic of this kind of radiation that, when dispersed by a prism or other similar means, a continuous spectrum is formed. In order that thermal radiation[6] may become visually observable, it is necessary that the temperature of the radiator should be 500 to 550°C. or above.

In 1879 Stefan, on the basis of the data observed by Tyndall, was led to suggest that the total emissive power of any body is proportional to the fourth power of the absolute temperature. Tyndall had shown that the ratio of the radiation from a platinum wire at 1200°C. to the radiation of the same wire at 525°C. was 11.7:1. Stefan pointed out that the ratio (24)

$$\frac{(1,200 + 273)^4}{(525 + 273)^4} = 11.6$$

[6]Hereafter thermal radiation will be called simply radiation, the adjective being omitted to save repetition.

thus indicating

$$W_{pt} = \sigma_{pt} T^4 \tag{4}$$

Boltzmann later (1884) deduced the same law from theoretical considerations by applying the laws of Carnot's cycle to the radiation in an "ether engine", the radiation playing the part of the working substance. The equation

$$W_B = \sigma T^4 \tag{5}$$

(W_B being the emissive power of a black surface) is known as the Stefan-Boltzmann law; and the proportionality constant σ is known as the Stefan-Boltzmann constant. This constant has the following values in the indicated units

0.173×10^{-8} BTU/(sq. ft.)(hr.)(deg. K)^4;
5.71×10^{-5} ergs/(sq. cm.)(sec.)(deg. K)^4;
4.92×10^{-8} Kg - cal/(sq. m.)(hr.)(deg. K)^4.

Equation (5) and its modifications may be considered the "working" equation for the engineering calculations of radiation transfer. Other properties of interest of black body radiation are its distribution in the spectrum and the shift of that distribution with temperature. If W_{B_λ} is the monochromatic emissive power at wave length λ such that $W_{B_\lambda} d_\lambda$ is the energy emitted from a surface throughout a hemispherical angle per unit area per unit time in the wave length interval λ to $\lambda + d\lambda$, the relation between W_{B_λ}, λ, and T is given by Planck's law.

$$W_{B_\lambda} = \frac{2\pi hc^2 \lambda^{-5}}{e^{ch/k\lambda T} - 1} = \frac{C_1 \lambda^{-5}}{e^{C_2/\lambda T} - 1} \qquad (6)$$

where c = velocity of light, 2.9979×10^{10} cm/sec;
h = Planck's constant, 6.6236×10^{-12} erg - sec;
k = Boltzmann's constant, 1.3802×10^{-16} erg/deg K;
$C_1 = 3.7403 \times 10^{-5}$ erg cm^2/sec; $C_2 = 1.4387$ cm deg K. The maximum of the Planck equation is given by Wien's Displacement Law

$$\lambda_{max} T = 0.2898 \text{ cm deg}^{\circ}\text{K}. \qquad (7)$$

This relation was observed by Wien before the introduction of the quantum theory in 1900. The wave length of maximum intensity is seen to be inversely proportional to the absolute temperature; therefore one would expect the larger part of the energy to be at the longer wave lengths at low temperatures. Figure 1 is a plot of energy versus wave length at approximately room temperature (300°K.) This figure emphasizes the point mentioned in Chapter I, that is, that visual observation may be erroneous at times. Notice that the maximum of the energy distribution is at approximately 9.7 microns, whereas the visible region observable by the eye is from 0.4 microns to 0.7 microns.

Emissivity and Absorptivity of Surfaces.--The emissivity (e) of a surface is defined at the ratio of the emissive power of that surface to the emissive power of a black surface at the same temperature. The absorptivity (α)

Figure 1

Energy Distribution of Black Body Radiation

$T = 300^{\circ}K.$

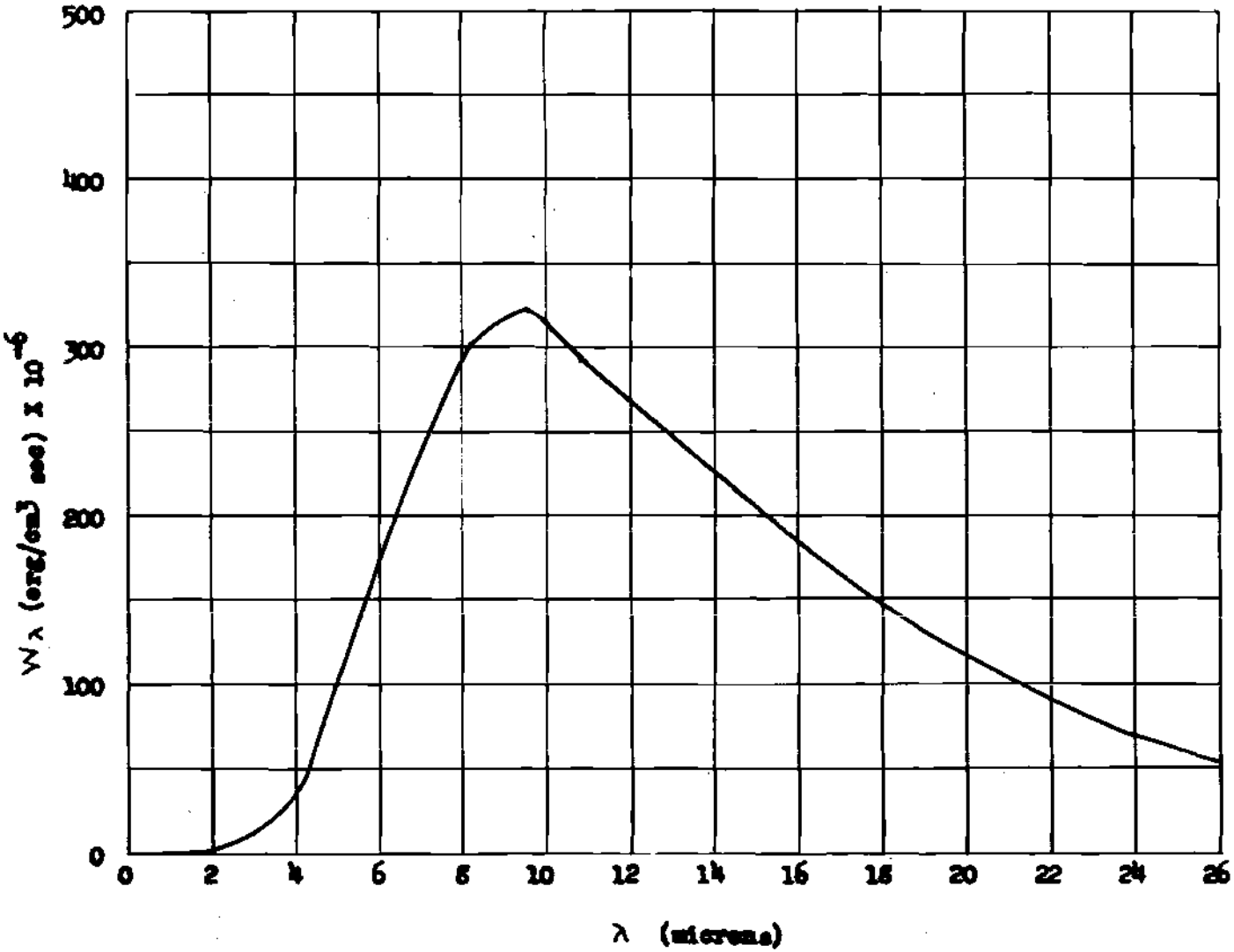
500
400
300
200
100
0
0
2
4
6
8
10
12
14
16
18
20
22
24
26
λ (microns)

and emissivity are related by Kirchhoff's law, which states that at thermal equilibrium the emissivity and absorptivity of a body are the same (23). Factors affecting the emissivity of a surface are temperature, degree of roughness, cleanness, and, if a metal, degree of oxidation. The absorptivity (α) of a surface depends on the same factors and, in addition, on the quality of the incident radiation, measured by its distribution in the spectrum. If α is a constant independent of λ , the surface is called gray and its total absorptivity (α) will be independent of the spectral-energy distribution of the incident radiation; then $\alpha_{12} = \alpha_{11} = e_1$; that is, emissivity (e) may be used in substitution for α even though the temperature of the incident radiation and the receiver are not the same. Only with the assumption of gray bodies can one calculate the emissivity of one surface knowing the emissivity of another at a different temperature and the heat transferred.

Radiant Interchange Between Two Gray Sources.--For radiant interchange between two surfaces forming part of an enclosure in the presence of a nonabsorbing medium, considerations of two kinds have to be made (1) the view the surfaces have of each other and (2) their emitting and absorbing characteristics. The only case in which the first of these need not be considered is the case of two infinite parallel planes since in this instance each surface has an unobstructed view of the other alone. The steps for the summation of the infinite geometric series for this case will not be given

since this summation can be found in most radiation texts (23). The result of this summation is

$$Q_{12} = A_1 \sigma (T_1^4 - T_2^4) \frac{1}{1/e_1 + 1/e_2 - 1} \tag{8}$$

In the case of radiant interchange between two gray finite parallel bodies without refractory surfaces, the view or configuration factor (F) must be considered. The configuration factor introduced by Langmuir, Adams, and Meikle (25) assumes that the intensity varies as the cosine of the angle from the normal of one source to the other, which is Lambert's cosine law. Making use of the configuration factor, one can proceed to solve this case. The fraction (per unit area) received by source A_2 from source A_1 will be $F_{12}\ e_1$ and the fraction reflected by source A_2 will be $F_{12}\ e_1\ (1 - e_2)$. The first reflection from A_1 will be $F_{12}^2\ e_1\ (1 - e_1)\ (1 - e_2)\ F_{21}$ and the second reflection from A_2 will be $F_{12}^2\ F_{21}\ (1 - e_1)\ (1 - e_2)^2$. This will proceed indefinitely. The summation of this infinite geometric series (see Appendix A) is

$$\frac{F_{12}\ e_1\ e_2}{1 - F_{12}\ F_{21}\ (1 - e_1)\ (1 - e_2)} \tag{9}$$

An exactly similar result applies for the fraction lost by A_2 except that F_{12} is replaced by F_{21} in the numerator of Equation (9). Since $A_1\ F_{12} = A_2\ F_{21}$ (see Reference 23, page 65) it follows that the net heat

absorbed by A_2 is given by

$$Q_{12} = \frac{F_{12}\, e_1\, e_2\, A_1}{1 - F_{12}\, F_{21}\, (1 - e_1)\, (1 - e_2)}\, \sigma\, (T_1^4 - T_2^4) \quad (10)$$

From the relation above it is obvious that when both sources are black ($e_1 = e_2 = 1$), the radiant transmission depends only on the configuration factors. One can rewrite Equation (10) in the form

$$Q_{12} = \mathcal{F}_{12}\, A_1\, \sigma\, (T_1^4 - T_2^4) \quad (11)$$

where $\mathcal{F}_{12}$ is an overall interchange factor. If refractory walls are present, the equation above is not valid. But the new overall interchange factor will still be some function of the configuration factors and the emissivities. Hottel gives a discussion of this situation (23).

Equation for the Cryostat Used in this Thesis.--A schematic diagram of the cryostat used in the radiation studies described in this thesis is shown in Chapter III, Figure 4. The section of the cryostat of immediate concern in the radiation studies is shown in Figure 2, where the principal radiating surfaces are indicated. Only the small tubes with area A_t are not indicated. The prime on the area of the outer cylinder wall (A_1') and the area of the inner cylinder wall (A_2') were so designated only to avoid confusion because of the use of A_1 and A_2 in the previous derivation. For the special case of this cryostat, a form of Equation (11)

Figure 2

Geometry of Radiating Surfaces of Cryostat

The surfaces A_1', A_3 and A_5 are the hot surfaces (273°K).
The surfaces A_2' and A_4 are the cold surfaces (77.4°K).
This figure is drawn to scale (1 in. = 1 in.).

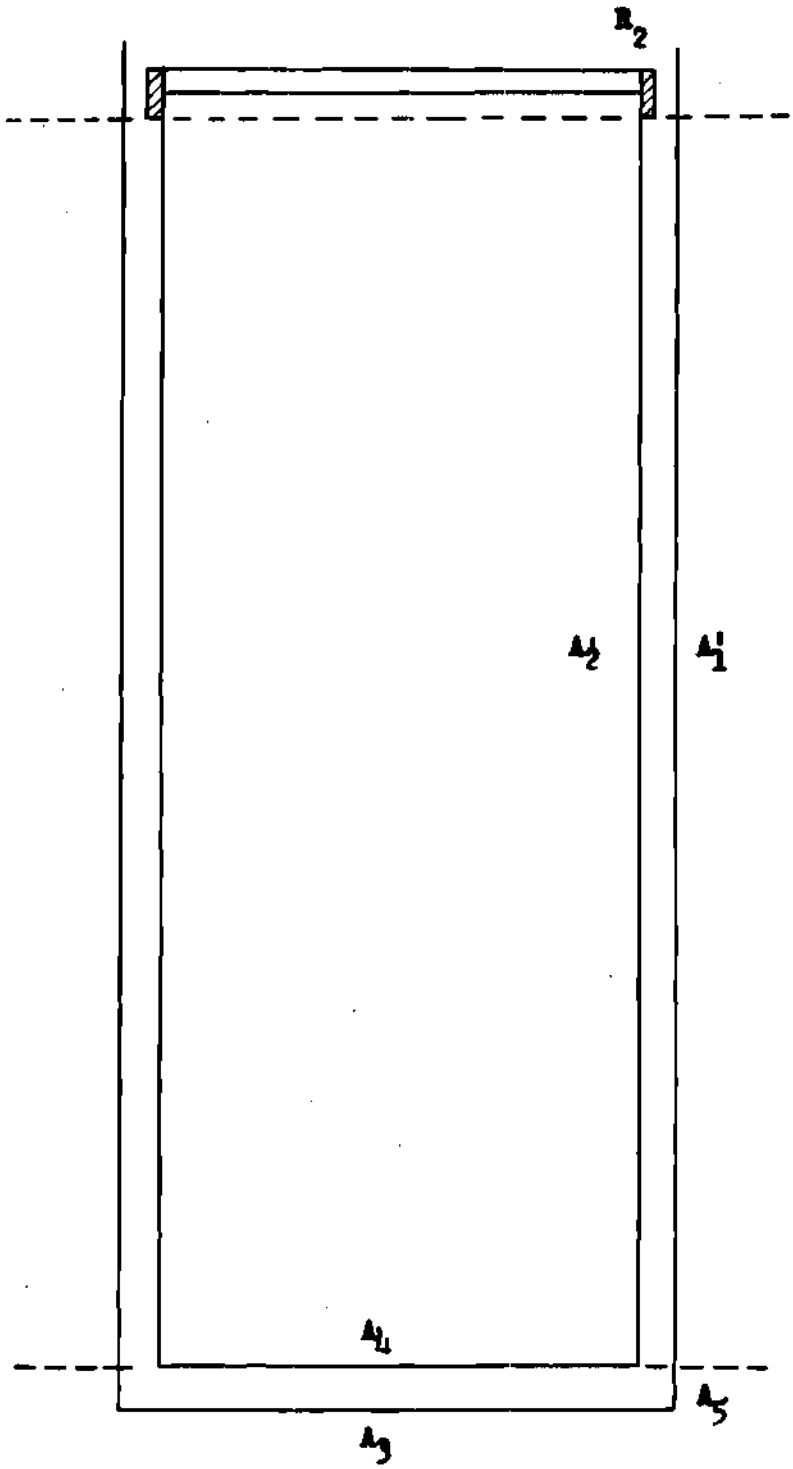
R2
A2
A'1
A4
A5
A3

is valid. But because of the complexity of the geometry, there is no known exact solution for this problem. In order to evaluate the $\mathcal{F}_{12}\ A_1$ term in Equation (11), this problem was resolved into 5 parts:

(1) Radiation transfer between A_1' and A_2'

(2) Radiation transfer between A_3 and A_4

(3) Radiation transfer between A_5 and A_4

(4) Radiation from the tubes (A_t)

(5) Radiation from A_5 to A_2' and A_3 to A_2'

Part (5) was neglected since the radiating sources are small and are never normal to the receiving sources. The sources A_1', A_3, and A_5 have the same emissivity (e_1). The emissivities of A_2' and A_4 are equal and will be represented by e_2. In order to simplify the mathematics, only the derivations for the absorbed fraction at A_2' and A_4 will be presented. The fraction lost by these sources have similar solutions and can be related as before (see page 17) since $A_2' F_{21} = A_1' F_{12}$, $A_4 F_{43} = A_3 F_{34}$, and $A_4 F_{45} = A_5 F_{54}$.

Radiation Transfer Between A_1' and A_2'.--This is a case of two concentric finite cylinders, the geometric solution of which has been determined by Hamilton and Morgan (26). The energy transfer consists of two parts, the diffuse radiation, which is the radiation that misses per reflection but scatters at the outer wall and does reach the inner surface on the next reflection, and the direct radiation from the outer surface to the inner surface.

Consider first the direct radiation. A_2' will receive

the fraction $F_{12}\ e_1$ from A_1' and A_2' will reflect $F_{12}\ e_1\ (1 - e_2)$. Of the fraction $F_{12}\ e_1\ (1 - e_2)$ reflected from A_2', $F_{12}^2\ F_{21}\ e_1\ (1 - e_1)\ (1 - e_2)$ will be received by A_2' again after reflection from A_1'. Then the fraction $F_{12}^2\ F_{21}\ e_1\ (1 - e_1)\ (1 - e_2)^2$ is reflected. The summation of the received fraction minus the summation of the reflected fraction is given by Equation (9)

$$\frac{F_{12}\ e_1\ e_2}{1 - F_{12}\ F_{21}\ (1 - e_1)\ (1 - e_2)}$$

The indirect diffuse radiation will now be considered. The fraction of the energy received from A_1' by A_2' from the first diffuse reflection is $F_{11}\ F_{12}\ e_1\ (1 - e_1)$. The reflected fraction from A_2' is $F_{11}\ F_{12}\ e_1\ (1 - e_1)\ (1 - e_2)$. These reflections will proceed indefinitely. The summation of the fraction absorbed which is the summation of the received fraction minus the summation of the reflected fraction (see Appendix B) is

$$\frac{F_{11}\ F_{12}\ e_1\ e_2\ (1 - e_1)}{1 - F_{12}\ F_{21}\ (1 - e_1)\ (1 - e_2)} \simeq q \qquad (12)$$

Let this diffuse quantity equal q.

Each direct reflection from A_2' also gives an indirect diffuse reflection, so the indirect radiation is

$$\frac{F_{12}\, e_1\, e_2}{1 - F_{12}\, F_{21}\, (1 - e_1)\, (1 - e_2)} \cdot q \qquad (12.1)$$

The total fraction of the radiation from the outer surface (A_1') to the inner surface (A_2') becomes

$$\frac{F_{12}\, e_1\, e_2}{1 - F_{12}\, F_{21}\, (1 - e_1)\, (1 - e_2)} (1 + q) \qquad (13)$$

which is the sum of Equations 12 and 12.1. It can be shown that there is a similar solution for the total fraction lost by A_2'.

Radiation Transfer Between A_3 and A_4.--The overall interchange factor between A_3 and A_4 has the same form as Equation (9) if A_3 and A_5 are assumed to have no effect upon each other, or in other words if A_3 approximately absorbs all energy striking it from A_5 and vice versa (see Appendix B).

Radiation Transfer Between A_5 and A_4.--The overall interchange factor between A_5 and A_4 has the same form as Equation (9). An additional assumption was made. The geometry of the case of radiant interchange between a perpendicular ring source to a circular disk has not been determined. The case of radiant interchange between a perpendicular element of area (dA) to a circular disk has been determined by Hamilton and Morgan (26). It is assumed that this case approximates the actual one (see Appendix B).

Radiation Transfer From the Tubes (A_t).--The radiant energy

from the apertures of the tubes leading into the sample container was considered black body radiation.

Total Radiation Transfer.--The total radiation transfer, which is the sum of all four of the net transfers (see Appendix B for complete derivation), is

$$Q = \left[\frac{F_{12}\, e_1\, e_2\, A_1'}{1 - F_{12}F_{21}(1 - e_1)(1 - e_2)} \left(1 + \frac{F_{11}\, F_{12}\, e_1\, e_2 (1 - e_1)}{1 - F_{12}F_{21}(1 - e_1)(1 - e_2)} \right) + \frac{F_{34}\, e_1\, e_2\, A_3}{1 - F_{34}F_{43}(1 - e_1)(1 - e_2)} + \frac{F_{54}\, e_1\, e_2\, A_5}{1 - F_{54}F_{45}(1 - e_1)(1 - e_2)} + A_t \right] \sigma \left(T_1^4 - T_2^4 \right) \qquad (14)$$

Application of Equation (14) to the Cryostat.--The conditions appropriate to this problem are:

$A_1' = 377.2\ cm^2$
$A_2' = 330.8\ cm^2$
$A_3 = 41.7\ cm^2$
$A_4 = 31.7\ cm^2$
$A_5 = 14.5\ cm^2$
$A_t = 0.25\ cm^2$
$T_1 = 273^\circ K$
$T_2 = 77.4^\circ K$

$F_{11} = 0.119$[7]
$F_{12} = 0.881$
$F_{21} = 1$
$F_{34} = 0.67$
$F_{43} = 0.882$
$F_{45} = 0.065$
$F_{54} = 0.142$
$e_1 = 0.866$

[7]All F factors taken from Hamilton and Morgan (26).

The emissivity (e_1) of the outer surface at the temperature of 273°K was determined by data obtained in Runs 2 and 12 (see Appendix C) with the assumption of gray surfaces. A complete discussion is given in Chapter IV. The final form of the equation after substitution in Equation (14) is

$$Q = 0.452 \left[\frac{288\ e_2}{1 - 0.118\ (1 - e_2)} \left(1 + \frac{0.0122\ e_2}{1 - 0.118\ (1 - e_2)} \right) + \right.$$

$$\left. \frac{24.2\ e_2}{1 - 0.0792\ (1 - e_2)} + \frac{1.78\ e_2}{1 - 0.00124\ (1 - e_2)} + 0.25 \right] \quad (15)$$

where Q has the units, calories per minute. A graphical solution (Figure 3) of Equation (15) can be obtained for Q and e_2.

It is obvious from the above equation that the first term, that for the cylindrical portion, is controlling, which is what one would expect from an observation of the magnitude of the radiating areas.

Figure 3

Graphical Solution of Equation (15) for Cryostat

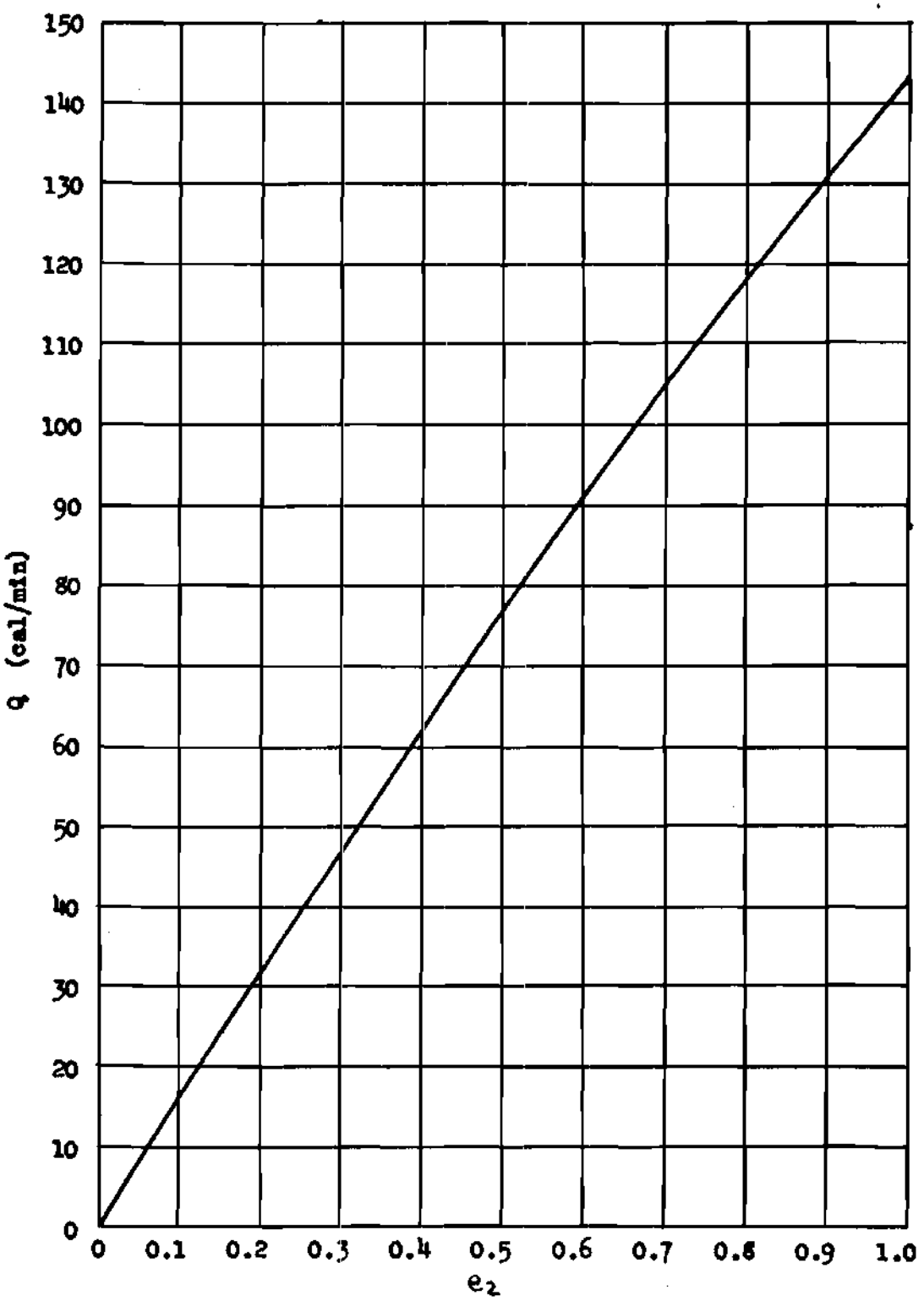
150
140
130
120
110
100
90
80
70
60
50
40
30
20
10
0
q (cal/min)
0
0.1
0.2
0.3
0.4
0.5
0.6
0.7
0.8
0.9
1.0
e_2

CHAPTER III

EXPERIMENTAL PROCEDURE

Apparatus.--After considering the work of other investigators, it was decided to construct a cryostat as shown in Figure 4 for radiation measurements. This cryostat is similar in design to the glass cryostat used by Blackman et al. (2). During the construction of this cryostat, Dr. W. T. Ziegler, the director of the cryogenic laboratory here at the Georgia Institute of Technology, noted at the Cryogenic Conference in Boulder, Colorado, that a metallic reservoir type cryostat, somewhat similar to this cryostat, was being used by Reynolds et al. at the National Bureau of Standards Laboratory in Boulder, Colorado (15). One might say that this cryostat is similar in design to Blackman's glass cryostat and similar to the NBS cryostat in that it is made of metal.

The cryostat consist of three parts, (1) a top or liquefied gas reservoir section (R) through which the tubes from above passed, (2) a lower section (M, called the sample container) on which various surfaces at liquid nitrogen temperature are studied, and (3) an outer jacket (J) blackened with a lampblack[8] suspension in glyptal. The

---

[8]Lampblack, Rainbow Genuine Germantown Lampblack made by the Murray-Williams Color and Chemical Company, Maplewood, N. J.

Figure 4

The Cryostat

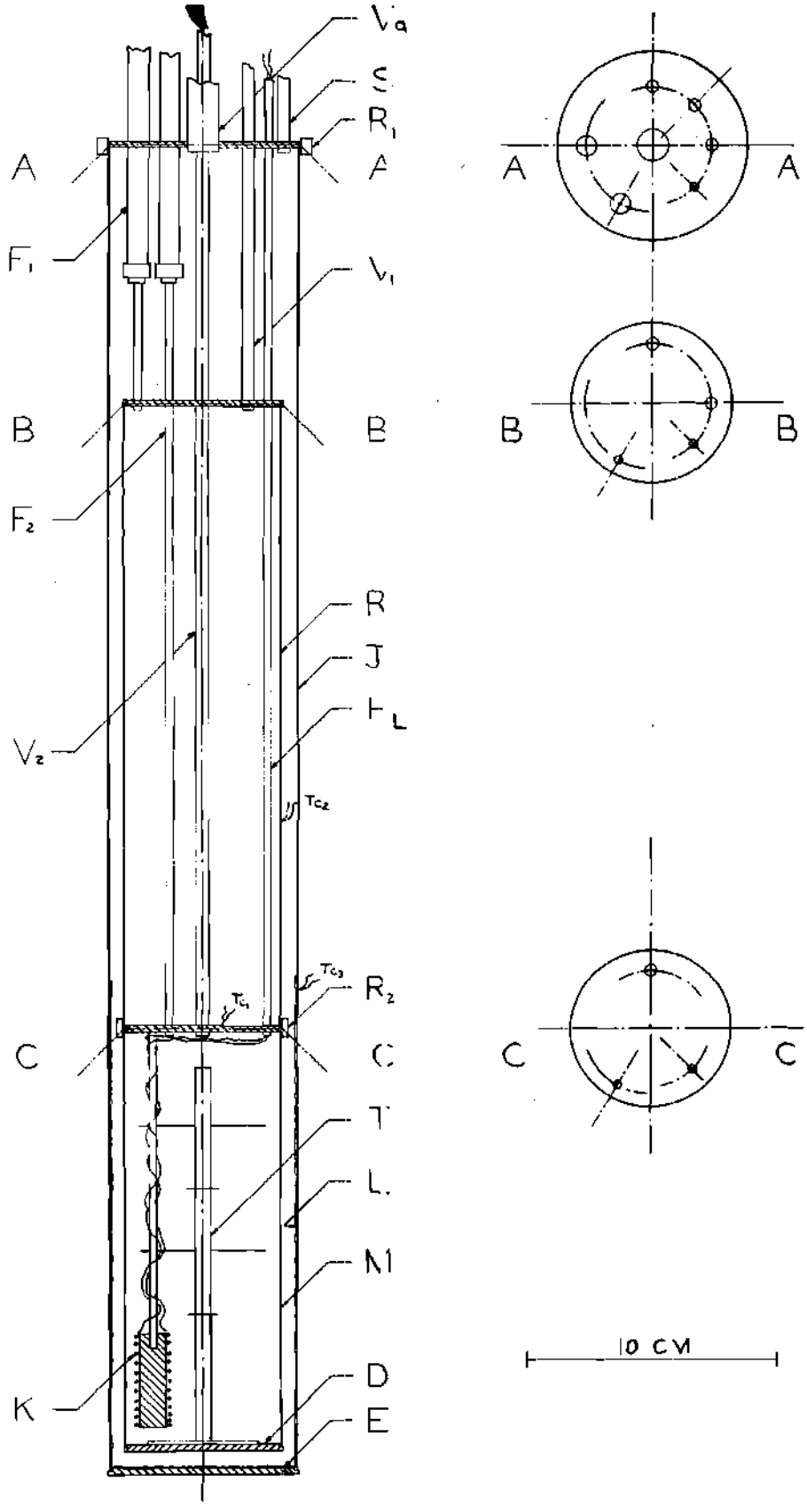
Va
S
R1
A
A
F1
V1
B
B
F2
R
J
FL
V2
Tc2
Tc3
R2
Tc1
C
C
T
L
M
D
K
E
A
A
B
B
C
C
10 CM

varnish coated the lower part of the jacket up to a height of approximately two inches above the sample container. The reservoir was designed to have sufficient refrigeration capacity so that the refilling of liquid nitrogen was unnecessary during an experiment. The reservoir was 2½ inches in outer diameter and 10 inches in length with a liquid storage capacity of 770 cubic centimeters. The reservoir was loosely wrapped with aluminum foil to minimize radiation heat leak. The sample container was 2½ inches in outer diameter and 6 5/8 inches long with a liquid capacity of 483 cubic centimeters for a monel container. The outer jacket had the dimensions, 3 inches outer diameter and 21 inches in length.

The materials of construction for the various parts are given in Table 1. All the joints of this cryostat are brazed with "Easy Flo" except for the tube joints at plate B and the joint connecting plate A and the outer jacket which are soldered with 40 Sn - 60 Pb solder. The sample container (M) was fastened to the reservoir (R) by means of Wood's metal at plate C.

Three sample containers which could be used interchangeably were made in order to conserve time in changing the surfaces. Two containers were made of monel metal (as indicated in Table 1) and one was made of free machining yellow brass. By using the brass sample container, the effect of changing the thermal conductivity of the sample

container could be studied.

A "tree" (T) made of copper sheet and brass rod was placed in the sample container to prevent superheating. The dimensions of each copper sheet were $\frac{1}{8}$ inch by 2 inches with a thickness of 0.01 inches. The rod was $\frac{1}{4}$ inch in diameter and 6 inches long. The rod support was a brass plate, 2 inches in diameter and 0.065 inches thick. Ten 20 cm. pieces of copper wire, 0.13 cm. in diameter were placed in the reservoir (R) for the same purpose of preventing superheating. The objective was to prevent a temperature gradient from existing across plate C.

Copper-Constantan thermocouples were connected to the cryostat in order to observe temperature changes throughout an experiment. Figure 5 is a wiring diagram of the various thermocouple connections. TC_1 was a difference couple. One junction was placed at the bottom of the reservoir and the other junction in a liquid nitrogen bath. Couple TC_2 had one junction fastened by solder to the outside of the reservoir approximately ten centimeters from ring (R_2) with the reference junction in an ice bath. Couple TC_3 was soldered to the outer jacket approximately twenty centimeters from the bottom with the reference junction in an ice bath. The EMF of each couple was observed with a Leeds and Northrup potentiometer (serial No. 707158) capable of estimating one microvolt. With these three thermocouples one is able to observe the temperature change of the outer

TABLE 1

Materials of Construction for Cryostat

Part	Material	Dimensions (in.)
Plate A at AA	Brass	3 Dia., 0.0936 Thick
Plate B at BB	Brass	2.5 Dia., 0.0936 Thick
Plate C at CC	Brass	2.5 Dia., 0.0936 Thick
Plate D	Monel	2.5 Dia., 0.0625 Thick
Plate E	Brass	3 Dia., 0.0936 Thick
Filling Tube (F_1)	Monel	1/8 x 0.01 Tube
Filling Tube (F_2)	Monel	1/8 x 0.01 Tube
Tube for (J)	Brass	3 x 0.065 Tube
Surface (L)	Lampblack	
Ring for (J)	Brass	3 I.D., 3.37 O.D. x 0.218
Ring for (M)	Brass	2.5 I.D., 2.95 O.D. x 0.25
Spare Line (S)	Monel	3/16 x 0.01 Tube
Vacuum Line (V_a)	Monel	$\frac{1}{8}$ x 0.01 Tube
Vent Line (V_1)	Monel	3/16 x 0.01 Tube
Vent Line (V_2)	Monel	3/16 x 0.01 Tube
Tube for (M)	Monel	2.5 x 0.035 Tube
Tube for (R)	Monel	2.5 x 0.035 Tube
Heater Line (H_L)	Monel	1/8 x 0.01 Tube

Figure 5

Electrical System

TC_1 = Thermocouple Junction No. 1

TC_2 = Thermocouple Junction No. 2

TC_3 = Thermocouple Junction No. 3

N = Liquid Nitrogen Bath

I = Ice Bath

S = Switch Board

P = Potentiometer

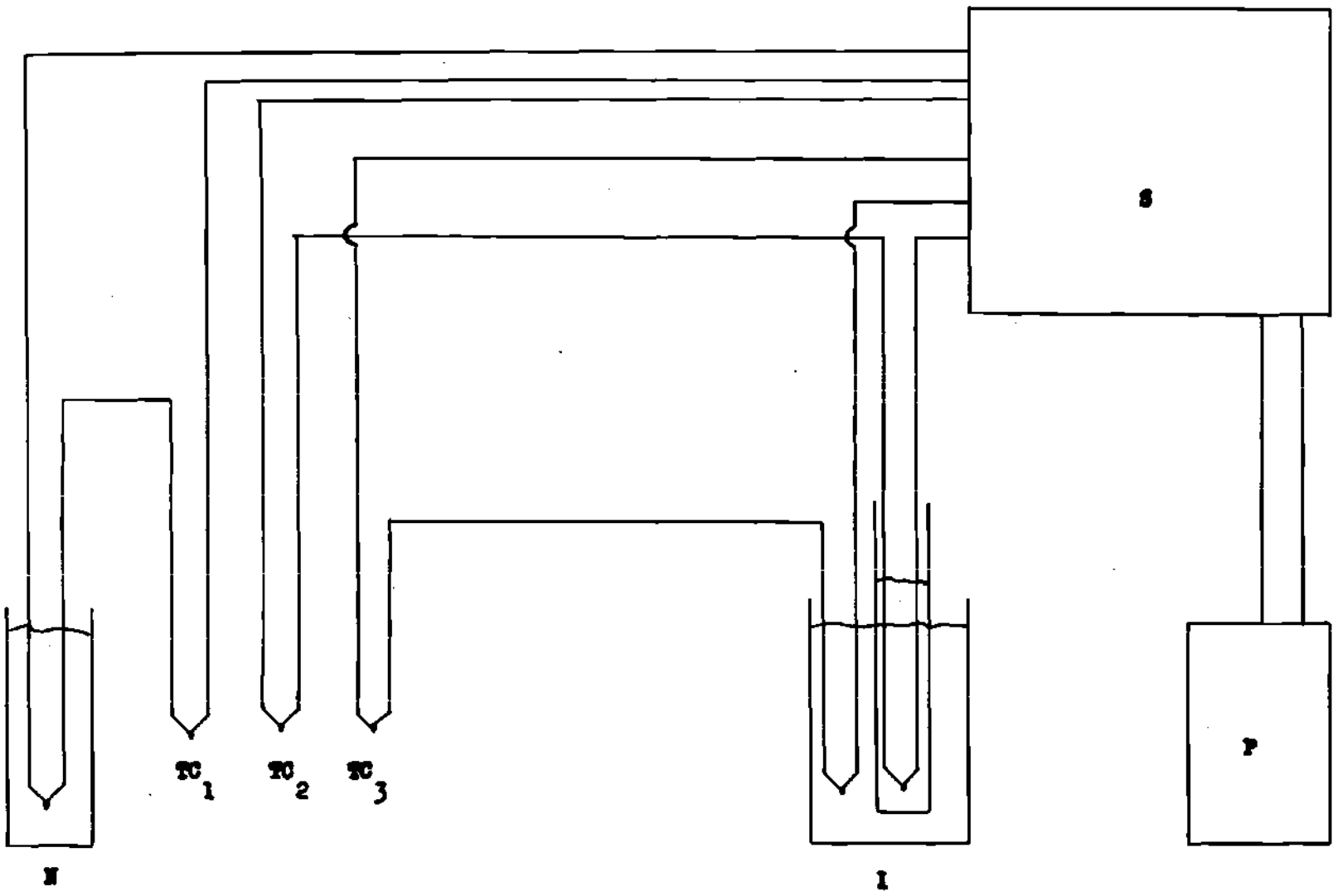
S
P
EC1
EC2
EC3
N
I

jacket, the liquid in the reservoir, and the wall of the reservoir. All the thermocouples were made of No. 34 copper and No. 32 Constantan wire.

A heater (K) was installed in the sample container. The purposes of this heater were to evaporate liquid nitrogen in the runs with low emissivity surfaces in order to obtain a check on the height measuring device and tc check the heat transfer. At high heat loads, the evaporation rate would be expected to become a linear function of heat input. By extrapolating to zero heat input, one is able to observe the "heat leaks" to the container and therefore have a check as to the value of the radiation transfer. The line of thought here is the same as that of Wexler's which was mentioned in Chapter I. Unfortunately, time did not permit experiments making use of this heater.

A height measuring device was installed in the vent line (V_2) for runs with low heat flux in order to conserve time. The height of the liquid nitrogen level in the high heat flux runs could be determined with a cumulative wet test meter since the time for the complete evaporation of the liquid in the sample container was reasonable (2-4 hours). The height measuring device mentioned above was used to measure the liquid level of the nitrogen in the sample container. This device will be referred to throughout this thesis as a probe. The probe consists of a thermocouple wrapped with a resistance heater attached to a 1/16 inch monel tube. The principle of this probe is quite simple.

As long as the thermocouple is in contact with the liquid nitrogen, the coefficient of heat transfer is large. Enough heat is removed to overcome the small amount of heat produced by the heater. Therefore, there will be no deflection of the potentiometer connected to the thermocouple. But when the thermocouple leaves the liquid, the coefficient of heat transfer diminishes greatly. This in turn will produce a sudden deflection in the potentiometer. By raising or lowering the probe one can determine approximately the gas-liquid interface. This probe is accurate to about 2 mm. in liquid height as determined by visual measurements made in a glass Dewar vessel.

The vacuum system briefly consists of a McLeod gauge (M), a diffusion pump (D), and two mechanical vacuum pumps (Me). The diffusion pump was a type VMV-20W made by the Consolidated Vacuum Company capable of maintaining an untimate pressure of $1 - 10^{-6}$ mm. Hg. with a forepressure of 0.100 mm. of Hg. The speed listed was 20 liters/min. at 1×10^{-4} mm. Hg. The two mechanical pumps were Duo-Seal vacuum pumps (115 volts, 60 cycles, A. C.) made by the W. M. Welch Manufacturing Company, capable of producing a vacuum of 0.0001 mm. Hg. The free-air capacity is 21 liters/min. A diagram of this system is shown in Figure 6.

Two flowmeters were used to measure the evaporation rates, one to measure the flow of evaporated gas from the sample container and another to measure the flow of evaporated gas from the reservoir. The flowmeter connected

Figure 6

Vacuum System

T_1 = Liquid Nitrogen Trap No. 1

T_2 = Liquid Nitrogen Trap No. 2

M = McLeod Gauge

U = U-Tube

D = Diffusion Pump

B = Mercury Bulb for U-Tube

Me_1 = Mechanical Vacuum Pump No. 1

Me_2 = Mechanical Vacuum Pump No. 2

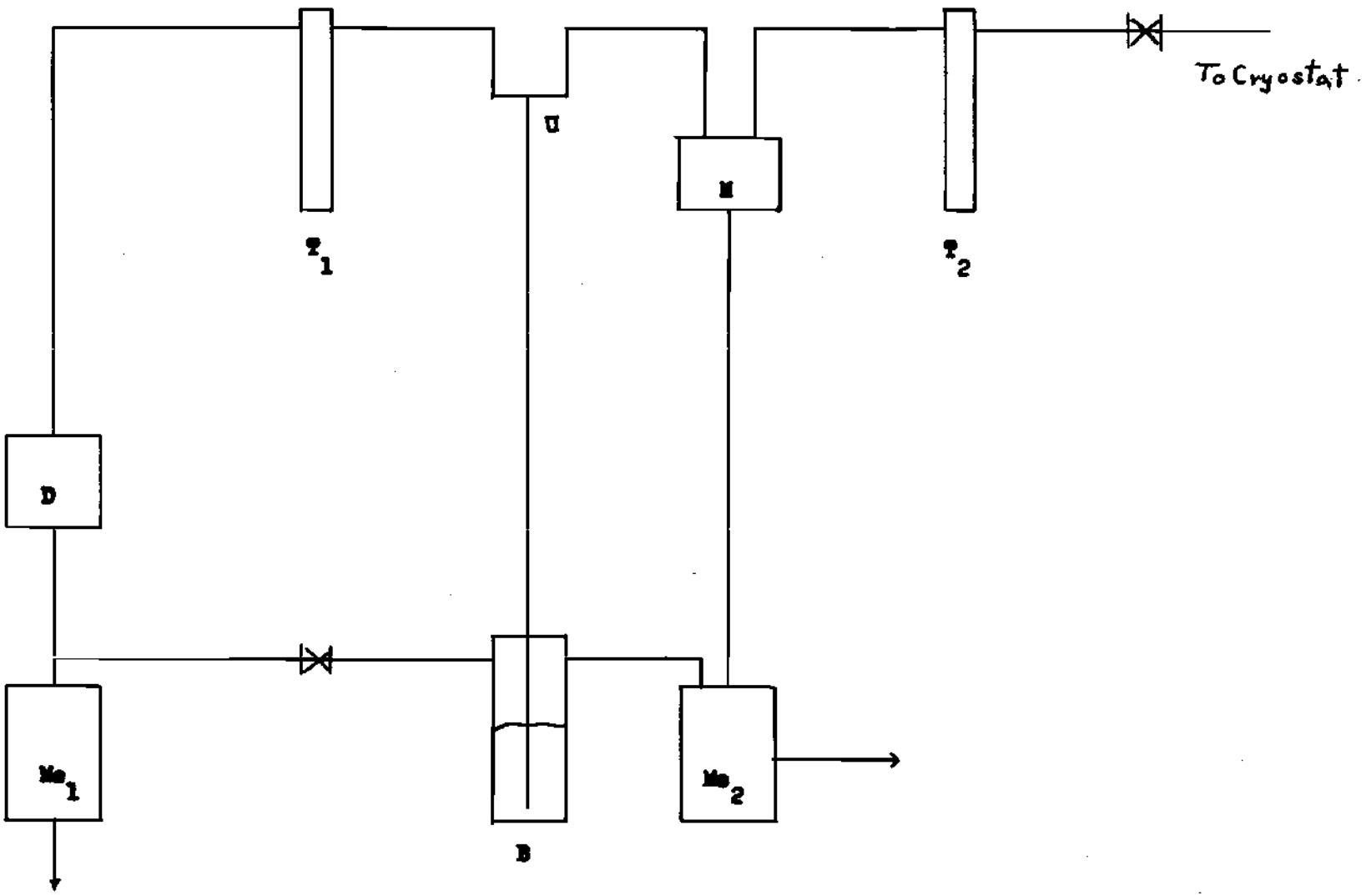
To Cryostat
U
M
P_1
P_2
D
Mo_1
B
Mo_2

to the sample container was the primary flowmeter. These were the measurements used in determining the heat transmission. This flowmeter and its connections etc. were considered the primary flowmeter system. A diagram of the primary flowmeter system is shown in Figure 7. The system was arranged in such a manner that an accumulative meter and an instantaneous meter could be operated in series at any time desired.

Three flowmeters were used in this experiment, two 20 cubic feet precision wet test meters and a capillary flowmeter made by the Scientific Glass Apparatus Company with three interchangeable capillaries. The capillary flowmeter that used dibutyl phthalate was the only flowmeter calibrated in this research. The capillary flowmeter was calibrated (see Appendix D for calibration) in such a manner that it could be used in series with a wet test meter. The two 20 cubic feet precision wet test meters were factory calibrated by the Precision Scientific Company, before purchase, with a rated accuracy of $\frac{1}{2}$ of one per cent. The two wet test meters were connected in series and a discrepancy of only 1/5 of one per cent was found. During various runs the capillary flowmeter and wet test meter were run in series; the maximum deviation noted was approximately two per cent.

Surfaces Studied.--This section of the thesis is devoted to a summary of the descriptions of the cold surfaces studied

Figure 7

Primary Flowmeter System

B = Saturation Vessel (20 Liters)

C = Water Manometer

D = Capillary Flowmeter

W = Precision Wet Test Meter

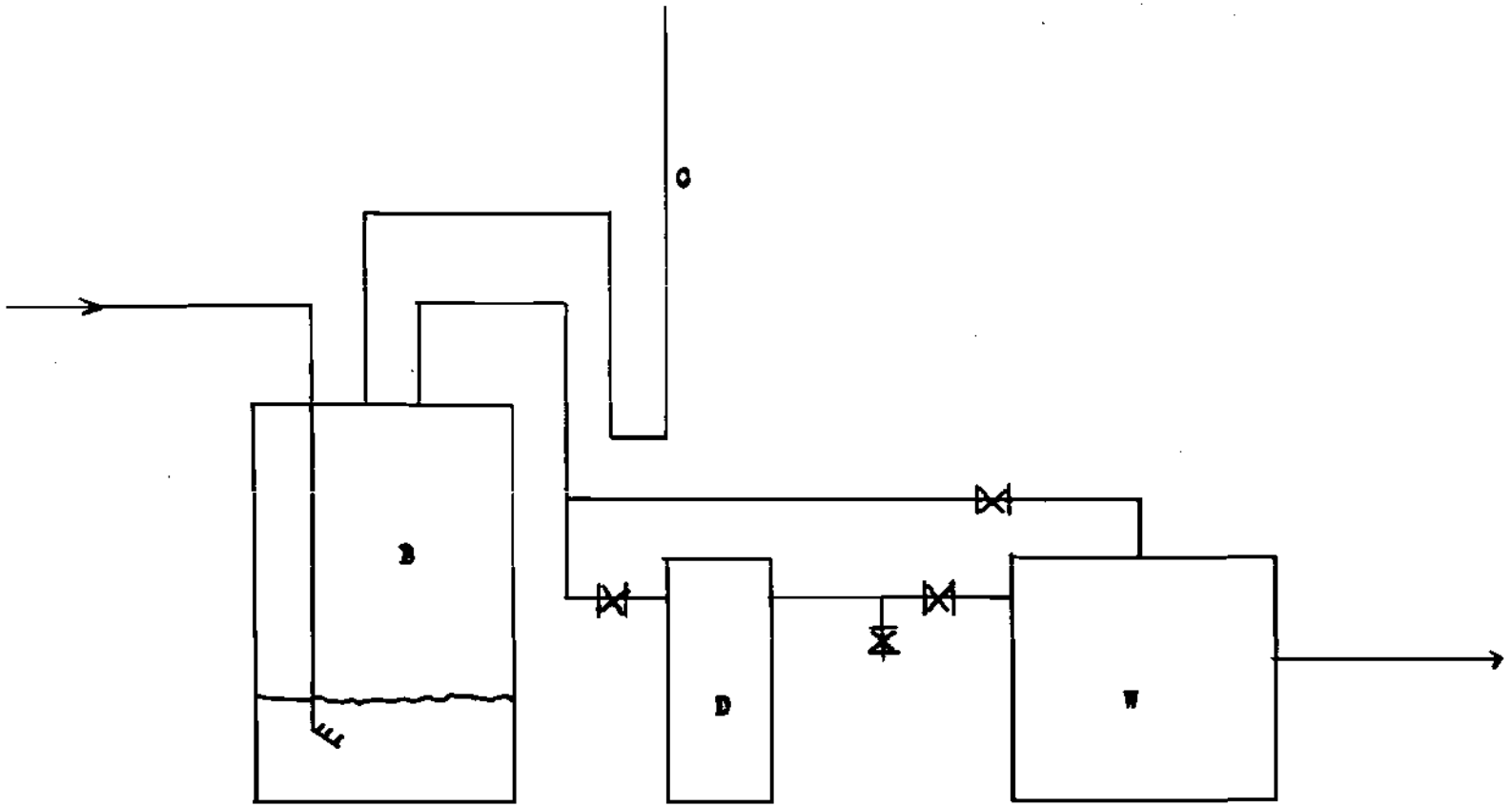
C
B
D
W
TE

in the runs summarized in Appendix C. After a study of the preliminary runs, it was decided that a suspension of 25 gm. of lampblack[9] in 60 cc. of glyptal (General Electric Company clear varnish No. 1202) and 30 cc. of thinner (G. E. No. 1500) would be suitable for the hot radiating surface (273°K.). The surface resulting after baking had the desired properties of good adhesion and roughness plus the fact that the surface was easy to degas.

A description of the various surfaces studied at liquid nitrogen temperature with the surface described above as the hot radiating surface are listed below:

(1) Lampblack - The lampblack-glyptal suspension after air drying overnight was baked at 125°C. for one and one half hours. This surface is the same as the hot surface as described above. The surface was black and very rough.

(2) Scotch Tape - A layer of Scotch Tape was wrapped on a monel container. The tape was two centimeters wide, clear, and transparent; but there were a few air bubbles in the surface.

(3) Brass - The free machining yellow brass tubing was hand-polished with No. 92 Crocus Cloth made by the Carborundum Company. The

---

[9]Lampblack, Rainbow Genuine Germantown Lampblack made by the Murray-Williams Color and Chemical Company, Maplewood, N. J.

resulting surface was bright and shiny with a few cuts.

(4) Monel - The monel container was polished in the same manner as the brass. The resulting surface was bright and shiny.

(5) Adhesive - General Electric Adhesive No. 7031 was brushed on a monel container. After air drying overnight, the coat of adhesive was transparent and had a brownish tinge.

(6) Aluminum Foil - Aluminum foil was loosely wrapped around a lampblack surface. The side exposed to the radiator had previously been polished by the manufacturer. (This was a household grade of foil produced by the Reynold's Company).

(7) Brass (tarnished) - The previous hand-polished brass (3) was tarnished in an oxidizing flame until the surface became dull. The surface had a brownish tinge. The oxidation was not uniform.

(8) Bakelite - A bakelite lacquer was air dried overnight and then baked at 135°C. for two hours. The resulting surface was non-uniform, brownish-red, and transparent. (This lacquer was an old batch of material used in a number of early cryostats).

(9) Wood's Metal - A coat of Wood's metal was applied to a brass container with a gas-air torch. The resulting surface was silver in color with a dull appearance. The surface was rough and not uniform.

(10) Chromium (plated) - Chromium was plated by a commercial plater on one of the monel containers. The resulting surface was bright, shiny, and uniform.

(11) Apiezon N - A thin film of Apiezon N grease was placed on the chromium plated surface of Run 15. The film of grease was very thin, uniform, and transparent.

(12) 40/60 Solder - A coat of 40 Sn - 60 Pb solder was placed on brass with a gas-air torch. The resulting surface was shiny and silvery in color but not uniform.

In the case of metals, no change in surface conditions were found after each run. In the case of non-metals (except for Apiezon N), the surfaces were cracked in every case. However, the adhesion of the varnish films to the sample container was good and no sign of flaking was observed.

Measurement and Interpretation.--The chronological operation of the apparatus described in this Chapter is as follows:

(1) Before each run the system was pumped overnight. The ultimate vacuum reached was approximately 1×10^{-5} mm. Hg.

(2) The reservoir and a sample container are filled with liquid nitrogen by means of a transfer device consisting of a two liter Dewar vessel, a nitrogen cylinder, and a vacuum insulated transfer tube. The reservoir was filled first.

(3) The sample probe was inserted into the sample container through the vent line. The height of the liquid nitrogen was recorded.

(4) The lines to the flowmeter systems were then connected. After these connections, the timer was started immediately.

(5) Flowrates at various times were recorded in the primary flowmeter system, which is connected to the sample container.

(6) Data such as barometric pressure, temperature of the outer jacket, temperature of the reservoir, and the vacuum pressure were then recorded and checked at various times during each experiment.

(7) The flowrate of the reservoir was observed at various times during the experiment in order to notice any superheating and to make a rough check with respect to the flowrate of the sample container. The initial flowrate of the reservoir corresponded to a heat leak of 12 cal./min. and increased throughout the experiment. The rate of increase in flowrate was approximately equivalent to the rate of decrease in flowrate in the sample container since the heat leak to the reservoir

was approximately a small constant rate plus the X factor effect of the sample container (see X factor effect in Chapter III).

From the data collected in step (5), a plot of flowrate versus time was made. Figure 8 is a plot of this type for Run 12 (see Appendix C for details). Knowing the height of liquid nitrogen in the sample container at the start either from the sample probe measurement or from the accumulative wet test meter measurement (if time is allowed for all the liquid nitrogen to evaporate), one can calculate the unfilled volume and the equivalent amount of gas for this volume. By extrapolating the flowrate-time curve allowing for this unfilled volume by graphical integration, the flowrate (R_r) corresponding to a full sample container can be determined. The integration can be done easily because of the straightness of the flowrate-time curve, and because of the shortness of the extrapolation. The container was approximately full at the start in every experiment.

Assuming the total heat flux to be radiation, one would expect an approximate linear relationship between the level of the liquid nitrogen (h) in the sample container and the flowrate since the flowrate is directly proportional to the heat transmitted. Consider Figure 9, the heat received (Q) is the sum of the heat flux from the end (Q_E) and from the cylinder up to the level of liquid nitrogen (Q_c') plus heat transmitted by conduction (XQ_c) which is some fraction X times the heat flux to the unfilled section. The relation

Figure 8

Flowrate Versus Time Plot for Run No. 12

Lampblack-Lampblack Surface

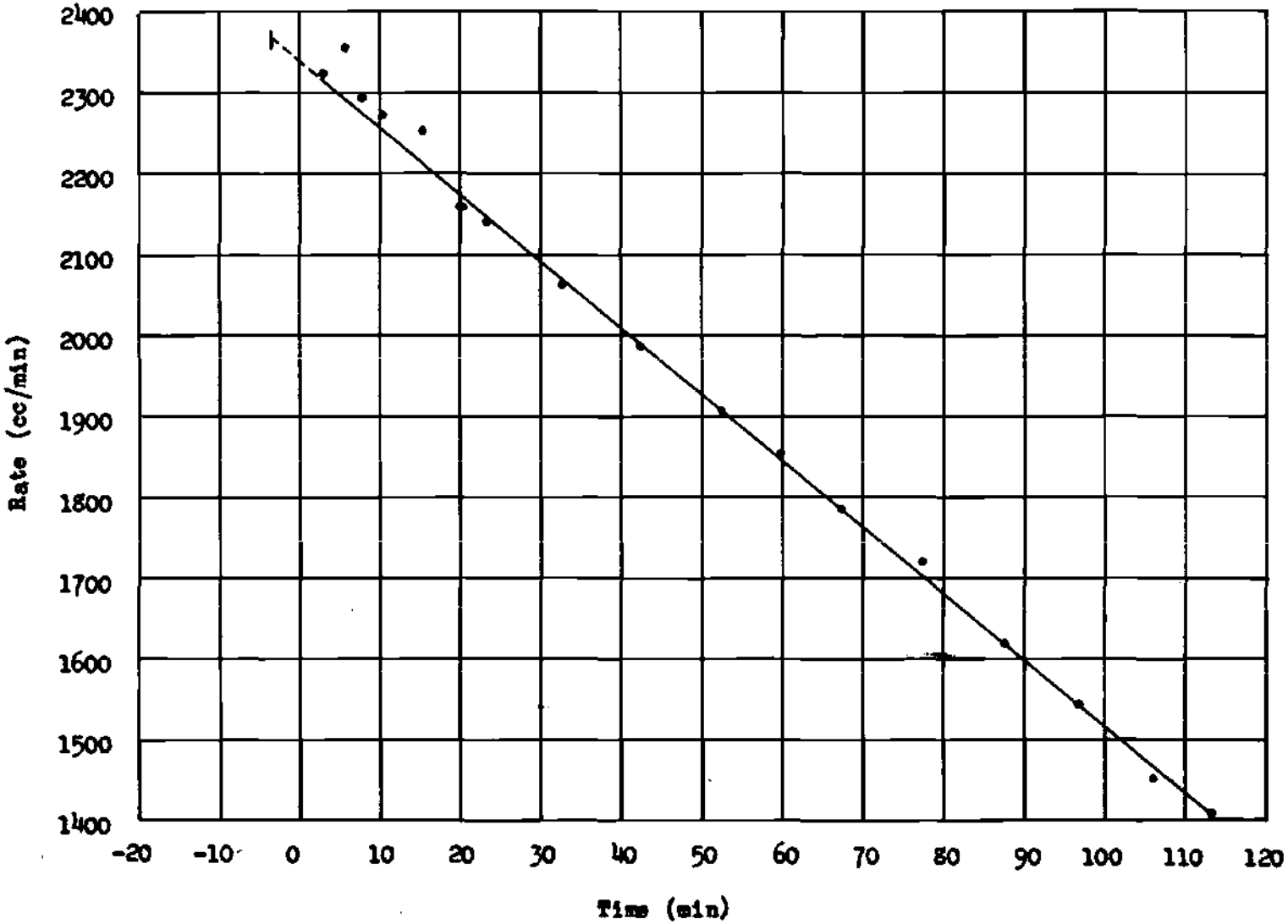
2400
2300
2200
2100
2000
1900
1800
1700
1600
1500
1400
Rate (cc/min)
-20
-10
0
10
20
30
40
50
60
70
80
90
100
110
120
Time (min)

Figure 9

Heat Flux to Sample

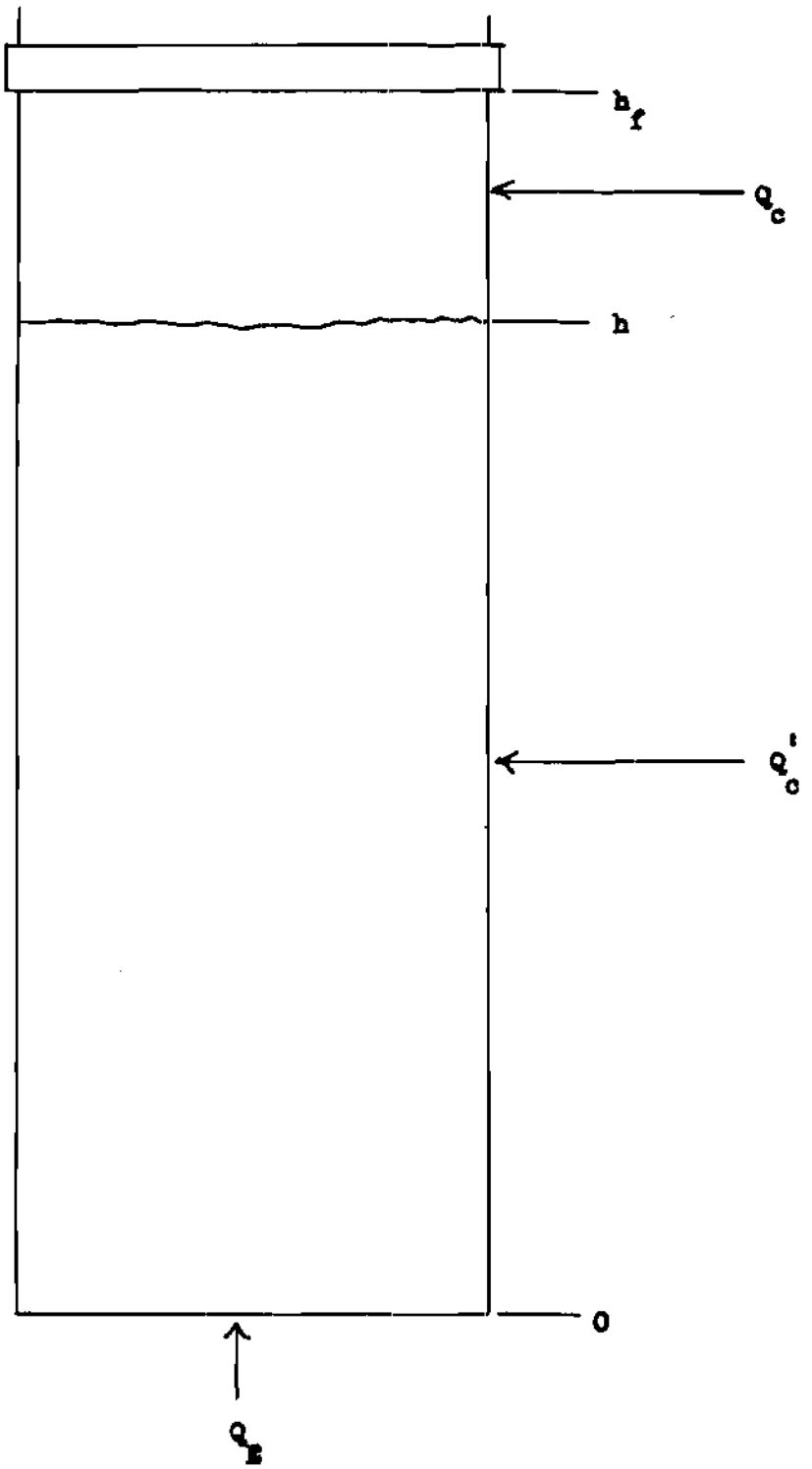
h_f
Q_c
h
Q_c'
0
Q_E

expressed mathematically is

$$Q = Q_E + XQ_c + Q_c' \tag{16}$$

Since the F factors, areas, and emissivities are constant for an experiment, one may express Equation (16) as follows

$$Q = Q_E + XK\,(h_f - h) + Kh \tag{17}$$

where K is a constant depending on the emissivities, areas, and the geometry (see Equation (14)). The full height (h_f) is 16.3 cm. Differentiating Equation (17) at constant X

$$dQ/dh = K\,(1 - X) \tag{18}$$

Therefore if X is constant, dQ/dh, which is directly proportional to the change in flowrate with time, is a constant. X should be a constant for a small drop in (h) because of the symmetry and the poor heat transfer to the evaporated gas. The fraction X was found to be in the neighborhood of 0.45 (see Appendix F for sample calculation). One would expect X to be 0.5, but evidently some energy was utilized in regard to the temperature rise of the unfilled portion of the sample container and perhaps some energy was transferred to the gas phase.

To obtain an emissivity (e_2) for the cold surface from a full flowrate (R_r), two assumptions in addition to the assumptions already made in Chapter II were made:

(1) The saturated nitrogen is an ideal gas mixture of nitrogen and water vapor.

(2) The pressure upon the liquid in the sample container is 760 mm. Hg.

With these two assumptions (see Appendix H for details)

$$Q = R_r\left(\frac{P_B}{P_o} \cdot \frac{T_o}{T} \cdot \frac{MW}{V_o} \cdot \frac{P_B - P_w}{P_B}\right) H_v \qquad (19)$$

where Q = net heat transmitted, cal/min.

P_B = Barometric pressure mm. Hg.

o = Subscript for standard conditions, P_o = 760 mm. Hg. $T_o = 273^oK$, V_o = 22,400 cc.

MW = Molecular weight of N_2, gm.

P_w = Vapor pressure of water at T, mm. Hg.

H_v = Heat of vaporization of N_2 at 760 mm. Hg., cal/gm.

R_r = Full flowrate, cc/min.

T = Temperature of gas, ^oK.

The bracket terms converted R_r (volume rate of flow) to a mass rate of flow. The latent heat of vaporization, 47.6 cal./gm. (27), times this quantity gives the heat transmission. Grouping the constant terms and simplifying, Equation (19) becomes

$$Q = C\, R_r \cdot \frac{P_B - P_w}{T} \qquad (20)$$

where C = constant = $0.002137 \frac{(Cal.)\ (^oK)}{(cc)(mm.\ Hg.)}$

When the capillary flowmeter was used, an additional term

was required to correct R_r to the conditions of the experiment since the calibrations of the capillaries were at a different temperature and pressure. This correction term for R_r is

$$\frac{P_B \cdot T_c}{P_{B_c} \quad T}$$

where the subscript c indicates the temperature and the barometer pressure of the calibration. This correction term is very small. A sample calculation applying the correction term is given in Appendix H. Once the full flowrate (R_r) is determined, one only has to substitute this value into Equation (20) for Q since P_B minus P_w and T are known for a specific run. Using the plot of Q versus e_2 in Chapter II, any e_2 can be determined depending on the full flowrate (R_r) of the sample. A sample calculation is given in Appendix H.

CHAPTER IV

DISCUSSION OF RESULTS

Results.--The results of this research are presented in Table 2.

TABLE 2

Summary of Results

Cold Surface (77.4°K)	Q (cal/min)	Per Cent Deviation	e_2
Lampblack in Glyptal	127.0	0.31 (2, 12)	0.866
Scotch Tape	130.4	1.76 (1, 3, 18)	0.89
G. E. Adhesive	128.8	(8)	0.88
Bakelite Lacquer	128.0	(11)	0.87
Brass	15.87	0.31 (4, 5)	0.098
Brass (tarnished	18.36	(10)	0.11
Monel	18.46	1.95 (6, 7)	0.11
Aluminum Foil	7.05	(9)	0.043
Chromium (plated)	13.85	0.29 (14, 15)	0.084
Wood's Metal	25.19	(13)	0.16
Apiezon N on Chromium	26.9	(16)	0.17
40 Sn - 60 Pb Solder	7.76	(17)	0.047

The radiating surface was lampblack in Glyptal at 273°K in all cases. The emissivity of the radiating surface was determined from data obtained in Runs 2 and 12 given in Appendix C. In both experiments, the radiating and the receiving surfaces were lampblack in Glyptal. Knowing the heat transfer from the evaporation rate and assuming gray bodies, the emissivity of the radiating and the receiving surfaces could be calculated from Equation (14) assuming $e_1 = e_2$. This

calculation is presented in Appendix H (also serves as sample calculation). Column 1 is the cold surface at 77.4°K. Column 2 is the rate of heat transmission assuming all energy transmitted to be radiant energy. For surfaces for which duplicate and triplicate runs were made, the rate of heat transmission is the average rate for all experiments performed with the surface. Column 3 is the per cent deviation in the rate of heat transmission between duplicates for a specific surface. In the case of a triplicate, the deviation of the extreme two was taken. The numbers in brackets following the percentage refer to the runs given in Appendix C. Column 4 is the apparent emissivity of the cold surface as calculated from Equation (15).

TABLE 3

Comparison of Several Common Surfaces

Material	Our (77.4°K)	Blackman (90°K)	Reynolds (76°K)
Brass	0.098	0.046	0.029
Aluminum Foil	0.043	0.055	0.02
Chromium	0.084	0.065	0.08
40/60 Solder	0.047		
50/50 Solder			0.03

Table 3 is a tabulation of common surfaces investigated by this research compared with the works of Blackman (2) and Reynolds (15). The large discrepancy in the apparent emissivity of brass is believed to be due to the different methods of polishing. The author did expect, however, that

the emissivity of brass and monel of this research would be high. In cleaning, grooves were made in the surface by the lathe. All the grooves could not be removed by hand polishing.

Accuracy of Results.--In Chapter I, seven "heat leaks" to Dewar vessels were listed:

(1) Conduction through the residual gas in the vacuum space.

(2) Convection through the residual gas in the vacuum space.

(3) Radiation across the vacuum space.

(4) Conduction along the neck of the flask.

(5) Radiation through the neck aperture.

(6) Conduction through supporting materials, if any, across the vacuum space.

(7) Convection in the interior space of the flask and neck.

Of these seven "heat leaks" only one of them, (1) conduction through the residual gas in the vacuum space, produced a significant error in the calculated apparent emissivities in Table 2. This error is in the neighborhood of 0.2 to 0.3 % for high emissivity surfaces and 2 to 3 % for low emissivity surfaces (see Appendix E for estimation of heat transmission by gaseous conduction). By the use of a high vacuum, small neck tubes, and a liquefied gas reservoir, all the other "heat leaks" can be assumed to be negligible except (3) radiation across the vacuum space and (5) radiation through the neck aperture. The assumption of blackbody radiation for the neck aperture accounts for (5).

The vacuum was 1 x 10^{-5} mm. Hg. The ratio of the areas of the tube apertures of the tubes leading to the sample container with respect to the total area of the sample container was approximately 1/2000. The assumption that the total "heat leak" is radiation is believed to be reasonable with the design of the apparatus used in this research.

The assumption of gray bodies for the calculation of the emissivity of the radiating surface is also believed to be reasonable. By decreasing the temperature of the radiating surface from 273.16°K to 194.2°K, using a Scotch Tape surface (Run 19) as the receiver, the observed heat transmitted was 31.1 cal./min. as compared with 32.4 cal./min. calculated by the temperature raised to the fourth power relationship. The deviation was four per cent. The precision of the system is believed to be two per cent, taking the precision equal to the reproduciability for the system. With a precision of two per cent for both rates of heat transmission, the deviation of four per cent is approximately within experimental error. It is believed that the lampblack surfaces are approximately gray.

Superheating of the reservoir was noted in a few of the experiments. The superheating was less than 0.10 C as observed by thermocouple measurements. However, this superheating seemed to have little effect upon the sample container since significant superheating would have made the X factor greater than 0.5.

The possibility of a temperature gradient existing across the plastic film of the radiating surface was also investigated. The analysis was made only on the outer surface since this surface was much more sensitive with respect to heat transmission. This is obvious because of the temperature to the fourth power relationship. A temperature gradient of 0.08°C (see Appendix G) was calculated for the radiating surface at 273°K and the gradient increased to 0.09°C for the same surface at 200°K. With an error of roughly four per cent per 1°C change in the radiating surface temperature at 273°K, the error produced by the temperature gradient across the radiating film is small.

No effect in the heat transmission was noted due to changing the thermal conductivity of the sample container from monel metal to yellow brass.

The experimental apparatus was found to approach the parallel plate case mentioned in Chapter II within less than two per cent (see Appendix I for discussion and calculation).

The limiting accuracy of the apparent emissivities in Table 2 is the assumption of Lambert's cosine law, the accuracy of which is in the neighborhood of 15 to 20 per cent. The author feels that the accuracy is within the accuracy of most chemical engineering calculations.

CHAPTER V

CONCLUSIONS AND RECOMMENDATIONS

In addition to the data presented, the author wishes to emphasize a few important facts which should be considered in the design of vacuum type containers or apparatus for low temperature use. It is obvious from the apparent emissivities obtained that plastics are good emitters and absorbers. Therefore, they should be shielded to minimize heat leak by radiation. Organic impurities will increase the emissivity. Generally speaking, most metallic surfaces are good reflectors. Aluminum foil is an excellent reflector. This material is of interest since it is very inexpensive and easy to handle. Polishing, cleaning, and maintaining a surface of low emissivity is expensive; but by wrapping aluminum foil upon any surface, one is insured of a reasonably low emissivity surface regardless of the contact of the aluminum foil to that surface. This method of decreasing the emissivity has industrial possibilities.

Some recommendations will be presented with respect to the apparatus used in this research. It is recommended that the reservoir section be constructed of a high thermal conductivity material in order to eliminate the small degree of superheating observed in the reservoir. Testing the grayness of some of the surfaces investigated in this

research is worthy of a master's thesis. This could be accomplished by the use of other liquefied gases such as helium, hydrogen, oxygen, and hydrocarbons for the cold surface temperature. Precaution, of course, will have to be taken if oxygen, hydrogen, or hydrocarbons are used. Some surfaces which one may use as standards for the above experiments are given in Table 4.

TABLE 4

Approximate Black Surfaces (77.4°K)

Surface	Apparent Emissivity
Scotch Tape	0.89
Bakelite Lacquer	0.87
G. E. Adhesive (No. 7031)	0.88
Lampblack in Glyptal	0.866

A tabulation of a few helpful emissivities for low temperature design in given in Table 5.

TABLE 5

Low Emissivity Materials

Material	Temp.(°K)	Emissivity	Reference
Silver	76	0.008	(15)
Polished Copper	76	0.03	(15)
Stainless Steel	76	0.048	(15)
Aluminum Foil	77.4	0.043	This Research
40 Sn/60 Pb Solder	77.4	0.047	This Research
Brass	90	0.046	(2)
Glass	90	0.87	(2)
Tin	90	0.038	(2)

APPENDIX A

DERIVATION OF OVERALL INTERCHANGE FACTOR

In the case of radiant interchange between two gray finite bodies without refractory surfaces, the view or configuration factor (F) must be considered in determining the overall interchange factor. Assuming two gray bodies A_1 and A_2, the fraction (per unit area) absorbed by source A_2 from A_1 is the difference of the received fraction and the reflected fraction at A_2.

Received by A_2 from A_1	Reflected from A_2
$F_{12}\, e_1$	$F_{12}\, e_1(1 - e_2)$
$F_{12}^2\, F_{21}\, e_1(1 - e_1)(1 - e_2)$	$F_{12}^2\, F_{21}\, e_1(1 - e_1)(1 - e_2)^2$
$F_{12}^3\, F_{21}^2\, e_1(1 - e_1)^2(1 - e_2)^2$	$F_{12}^3\, F_{21}^2\, e_1(1 - e_1)^2(1 - e_2)^3$

Sum of the Received is

$$F_{12}\, e_1 \left[1 + F_{12}\, F_{21}\, (1 - e_1)(1 - e_2) + F_{12}^2\, F_{21}^2\, (1 - e_1)^2 (1 - e_2)^2 + - - - - - - - - + F_{12}^{n-1} F_{21}^{n-1} (1 - e_1)^{n-1} (1 - e_2)^{n-1}\right]$$

which has the form

$$K\,(1 + X + X^2 + X^3 + - - - - - - - - X^{n-1})$$

the sum of which is

$$K\left(\frac{1}{1-X}\right)$$

therefore the summation of the received is

$$\frac{F_{12}\, e_1}{1 - F_{12}\, F_{21}\, (1 - e_1)\, (1 - e_2)}$$

The sum of the reflected is

$$F_{12}\, e_1\, (1 - e_2)\, \left[1 + F_{12}\, F_{21}\, (1 - e_1)(1 - e_2) + F_{12}^2\, F_{21}^2\, (1 - e_1)^2\, (1 - e_2)^2 + - - - - - - - - \right]$$

which has the same form as the series above. This summation is

$$\frac{F_{12}\, e_1\, (1 - e_2)}{1 - F_{12}\, F_{21}\, (1 - e_1)\, (1 - e_2)}$$

The difference of the former and the latter series is the fraction absorbed

$$\frac{F_{12}\, e_1\, e_2}{1 - F_{12}\, F_{21}\, (1 - e_1)\, (1 - e_2)} \qquad (9)$$

The fraction absorbed by source A_1 from A_2 obviously would give similar results except F_{12} and e_1 are replaced by F_{21}

and e_2, and vice versa, throughout the above derivation. The fraction absorbed at source A_1 would be

$$\frac{F_{21}\ e_2\ e_1}{1 - F_{21}\ F_{12}\ (1 - e_1)\ (1 - e_2)} \tag{9a}$$

The energy absorbed by A_2 is $\sigma A_1\ T_1^4$ times Equation (9) and the energy absorbed by A_1 is $\sigma A_2\ T_2^4$ times Equation (9a). Therefore, the net energy absorbed by A_2 is the difference of the former and the latter products.

$$Q_{12} = \frac{e_1\ e_2\ \sigma (F_{12}\ A_1\ T_1^4 - F_{21}\ A_2\ T_2^4)}{1 - F_{12}\ F_{21}\ (1 - e_1)\ (1 - e_2)} \tag{9b}$$

or since $F_{12}\ A_1 = F_{21}\ A_2$ (see reference (23), page 65) the above equation can be expressed

$$Q_{12} = \frac{F_{12}\ e_1\ e_2\ A_1}{1 - F_{12}\ F_{21}\ (1 - e_1)\ (1 - e_2)}\ \sigma (T_1^4 - T_2^4) \tag{10}$$

after substituting $F_{12}\ A_1$ for $F_{21}\ A_2$. The overall interchange factor $\mathcal{F}$ is Equation (9).

APPENDIX B

DERIVATION FOR EQUATION OF CRYOSTAT

The purpose of this appendix is to give a more complete derivation of Equation (15) since many mathematical steps were omitted in Chapter II. The notation will be the same.

The problem was resolved into five parts as was stated in Chapter II:

(1) Radiation transfer between A_1' and A_2'
(2) Radiation transfer between A_3 and A_4
(3) Radiation transfer between A_5 and A_4
(4) Radiation from the tubes (A_t)
(5) Radiation from A_5 to A_2' and A_3 to A_2'

Part (5) was neglected since the radiating areas are small and are never normal to the receiving sources.

Radiation Transfer Between A_1' and A_2'.--This is the case of two concentric finite cylinders, the geometric solution of which has been determined by Hamilton and Morgan. The energy transfer consist of two parts: the diffuse radiation which is the radiation that misses per reflection but scatters at the outer wall and does reach the inner surface on the next reflection, and the direct radiation from the outer surface

to the inner surface. The direct radiation from A_1' to A_2' is given by Equation (9) in Appendix A.

For the diffuse radiation, the following applies

Received by A_2' after diffuse reflection at A_1'

$$F_{11}\ F_{12}\ e_1\ (1 - e_1)$$

$$F_{11}\ F_{12}^2\ F_{21}\ e_1\ (1 - e_1)^2(1 - e_2)$$

$$F_{11}\ F_{12}^3\ F_{21}^2\ e_1\ (1 - e_1)^3(1 - e_2)^2$$

Reflected from A_2'

$$F_{11}\ F_{12}\ e_1\ (1 - e_1)\ (1 - e_2)$$

$$F_{11}\ F_{12}^2\ F_{21}\ e_1\ (1 - e_1)^2(1 - e_2)^2$$

$$F_{11}\ F_{12}^3\ F_{21}^2\ e_1\ (1 - e_1)^3(1 - e_2)^3$$

Sum of the received is

$$F_{11}\ F_{12}\ e_1\ (1 - e_1)\ \left[1 + F_{12}\ F_{21}\ (1 - e_1)\ (1 - e_2) + F_{12}^2\ F_{21}^2\ (1 - e_1)^2(1 - e_2)^2 + - - - - - - - -\right]$$

The summation of which is

$$\frac{F_{11}\ F_{12}\ e_1\ (1 - e_1)}{1 - F_{12}\ F_{21}\ (1 - e_1)\ (1 - e_2)}$$

The sum of the reflected is

$$F_{11}\,F_{12}\,e_1\,(1-e_1)\,(1-e_2)\,\left[1+F_{12}\,F_{21}\,(1-e_1)(1-e_2)+\right.$$
$$\left.F_{12}^2\,F_{21}^2\,(1-e_1)^2(1-e_2)^2+-\,-\,-\,-\,-\,-\right]$$

Summation of which is

$$\frac{F_{11}\,F_{12}\,e_1\,(1-e_1)\,(1-e_2)}{1-F_{12}\,F_{21}\,(1-e_1)\,(1-e_2)}$$

The difference, the absorbed fraction, is

$$\frac{F_{11}\,F_{12}\,e_1\,(1-e_1)\,e_2}{1-F_{12}\,F_{21}\,(1-e_1)\,(1-e_2)} \qquad (12)$$

The fraction absorbed by A_1' will give similar results except F_{12} in the above equation is replaced by F_{21}.

Received by A_1' (diffused)

$$F_{11}\,F_{21}\,e_2\,(1-e_1)$$

$$F_{11}\,F_{12}\,F_{21}^2\,e_2\,(1-e_1)^2(1-e_2)$$

Reflected from A_1'

$$F_{11}\,F_{21}\,e_2\,(1-e_1)^2$$

$$F_{11}\,F_{12}\,F_{21}^2\,e_2\,(1-e_1)^3(1-e_2)$$

The difference of the summations of the fraction received

and the fraction reflected which is the fraction absorbed by A_1' from A_2' is given by

$$\frac{F_{11}\, F_{21}\, e_1\, e_2\, (1 - e_1)}{1 - F_{12}\, F_{21}\, (1 - e_1)\, (1 - e_2)} \qquad (12a)$$

This expression then can be expressed with respect to A_1' by the substitution $A_1' F_{12} = A_2' F_{21}$ to give Equation (12). Let Equation (12) equal q. Since each term of the direct series has a diffuse summation, the total amount absorbed will be

$$\frac{F_{12}\, e_1\, e_2}{1 - F_{12}\, F_{21}\, (1 - e_1)\, (1 - e_2)}\ (1 + q)$$

Radiation Transfer Between A_3 and A_4.--This is the case of two parallel disk, one larger than the other, if A_3 and A_5 are assumed to have no effect upon each other, or in other words A_3 absorbs all radiation striking it from A_5 and vice versa. Then the fraction received by A_4 and the fraction reflected by A_4 are

Received by A_4 from A_3	Reflected from A_4
$F_{34}\, e_1$	$F_{34}\, e_1\, (1 - e_2)$
$F_{34}^2\, F_{43}\, e_1\, (1 - e_1)(1 - e_2)$	$F_{34}^2\, F_{43}\, e_1\, (1 - e_1)(1 - e_2)^2$
$F_{34}^3\, F_{43}^2\, e_1\, (1 - e_1)(1 - e_2)^2$	$F_{34}^3\, F_{43}^2\, e_1\, (1 - e_1)^2(1 - e_2)^2$

The sum of the received is

$$F_{34}\, e_1 \left[1 + F_{34}\, F_{43}\, (1 - e_1)(1 - e_2) + F_{34}\, F_{43}\, (1 - e_1)^2(1 - e_2) + - - - - - - - -\right]$$

The summation becomes

$$\frac{F_{34}\, e_1}{1 - F_{34}\, F_{43}\, (1 - e_1)\, (1 - e_2)}$$

The sum of the reflected is

$$F_{34}\, e_1\, (1 - e_2) \left[1 + F_{34}\, F_{43}\, (1 - e_1)(1 - e_2) + F_{34}^2\, F_{43}^2\, (1 - e_1)^2(1 - e_2)^2 + - - - - - - - -\right]$$

The summation of this series is

$$\frac{F_{34}\, e_1\, (1 - e_2)}{1 - F_{34}\, F_{43}\, (1 - e_1)\, (1 - e_2)}$$

The fraction absorbed being the difference of the former series and the latter series is

$$\frac{F_{34}\, e_1\, e_2}{1 - F_{34}\, F_{43}\, (1 - e_1)\, (1 - e_2)}$$

The fraction absorbed by A_3 can be treated as before making use of the relation $A_3\, F_{34} = A_4\, F_{43}$.

Radiation Transfer Between A_5 and A_4.--In addition to the assumption in (2), it is assumed that this case of a perpendicular ring radiating to a circular disk is approximately equal to the case of a perpendicular element of area (dA) to a circular disk. With these assumptions, the absorbed fraction is

$$\frac{F_{54}\, e_1\, e_2}{1 - F_{54}\, F_{43}\, (1 - e_1)\, (1 - e_2)}$$

The derivation of the absorbed fraction is the same as that of (2).

Radiation From the Tubes (A_t).--The radiant energy from the apertures of the tubes leading into the sample container is assumed blackbody radiation.

The final relationship for the heat transmission is

$$Q = \left[\frac{F_{12}\, e_1\, e_2\, A_1'}{1 - F_{12}F_{21}(1 - e_1)(1 - e_2)} \left(1 + \frac{F_{11}\, F_{12}\, e_1\, e_2 (1 - e_1)}{1 - F_{12}F_{21}(1 - e_1)(1 - e_2)} \right) + \frac{F_{34}\, e_1\, e_2\, A_3}{1 - F_{34}F_{43}(1 - e_1)(1 - e_2)} + \frac{F_{54}\, e_1\, e_2\, A_5}{1 - F_{54}F_{45}(1 - e_1)(1 - e_2)} + A_t \right] \sigma\, (T_1^4 - T_2^4) \qquad (14)$$

Substituting the conditions imposed by the cryostat,

$A_1' = 377.2\ cm^2$ $\quad F_{11} = 0.119$

$A_2' = 330.8\ cm^2$ $\quad F_{12} = 0.881$

$A_3 = 41.7\ cm^2$ $\quad F_{21} = 1$

$A_4 = 31.7\ cm^2$ $\quad F_{34} = 0.67$

$A_5 = 14.5\ cm^2$ $\quad F_{43} = 0.882$

$A_t = 0.25\ cm^2$ $\quad F_{45} = 0.065$

$T_1 = 273^\circ K$ $\quad F_{54} = 0.142$

$T_2 = 77.4^\circ K$ $\quad e_1 = 0.866$

The equation for the cryostat becomes

$$Q = 0.452 \left[\frac{288\ e_2}{1 - 0.118\ (1 - e_2)} \left(1 + \frac{0.0122\ e_2}{1 - 0.118\ (1 - e_2)} \right) + \right.$$

$$\left. \frac{24.2\ e_2}{1 - 0.0792\ (1 - e_2)} + \frac{1.78\ e_2}{1 - 0.00124\ (1 - e_2)} + 0.25 \right]$$

The configuration factors F_{11}, F_{34}, and F_{54}, were taken from Hamilton and Morgan (26). F_{11} (denoted as Configuration L-4 by Hamilton and Morgan, page 29) was evaluated from Table 11 (page 66 of the above reference). In order to avoid linear extrapolation, a large plot was produced using their 4 place factors. F_{11} was then taken to be the value found on this plot. The values were rounded off to 3 places. F_{34} (Configuration A-6, page 32 and Table 14, page 69 of (26)) was evaluated by the same means. F_{54} (Configuration

P-7, page 25 and Equation P-7 of Appendix C, page 37 of (26)) was evaluated from Equation P-7 of Hamilton and Morgan. F_{21} was assumed to be one. F_{12} was taken to be $1 - F_{11}$. F_{43} and F_{45} were evaluated from the relations, $F_{34} A_3 = F_{43} A_4$ and $F_{45} A_4 = F_{54} A_5$. In both cases, three of the values are known. The following reasoning is used. Assuming two black sources, A_x and A_y, the equation for the net heat interchange is

$$Q_{xy} = \sigma (F_{xy} A_x T_x^4 - F_{yx} A_y T_y^4)$$

Since the configuration factors are independent with respect to temperature, Q_{xy} will approach zero as T_y approaches T_x. Because σ is a constant, the relation

$$F_{yx} = F_{xy} \frac{A_x}{A_y}$$

is true. Therefore, if one knows one configuration factor, the other can be determined (knowing the areas of the two sources). Numbers used in the evaluation of F_{11}, F_{34}, and F_{54} are given below (notations same as that of Hamilton and Morgan).

Configuration L-4

$$D = d/r = \frac{1.435}{1.25} = 1.154$$

$$L = l/r = \frac{6.656}{1.25} = 5.325$$

$F_{11} = 0.119$ from Table 11, page 66 (26)

where d = outer cylinder radius

r = inner cylinder radius

l = length of cylinder

Configuration A-6

$E = r_2/d = \frac{1.25}{0.25} = 5$

$D = d/r_1 = \frac{0.25}{1.435} = 0.174$

$F_{34} = 0.67$ from Table 14, page 69 (26)

where d = distance between disks

r_1 = radius of larger disk

r_2 = radius of smaller disk

Configuration P-7

$R = \frac{r}{b} = \frac{1.25}{1.435} = 0.871$

$D = \frac{a}{b}$, varied from 0 to 0.174

$F_{54} = 0.142$ from Equation P-7, page 37 (26) assuming D to be zero and 0.174 and taking an arithmetic average of the two

where r = radius of perpendicular disk

b = vertical distance to plane containing dA_5 from center of perpendicular disk

a = horizonal distance from perpendicular disk to element of area dA_5

APPENDIX C

SUMMARY OF OPERATING DATA

This appendix is a summary of the information obtained from 3 preliminary and 19 experimental runs.

The hot surface indicated on the various data sheets is at a temperature of 273°K. The cold surface is at 77.4°K, the boiling point of nitrogen at 1 atm. The full flowrate (R_r) is the extrapolated flowrate corresponding to a level of 16.3 cm. in the sample container. The height from the bottom of the sample container to the lower edge of the brass ring is 16.3 cm. The height at start is the height of the liquid nitrogen at zero time. Zero time is the time at which the primary flowmeter system and the cryostat were connected. When wet test meter is indicated, this refers to the 20 cubic feet precision meter. When capillary is indicated, this means the capillary flowmeter was used. The number after the word capillary designates the capillary used. The flowrates given are for the primary flow system. At the bottom of each data sheet is a brief description of the cold surface. All other items are self-explanatory.

APPENDIX C

TABLE 6

Summary of Operating Data for Run 1

Hot Surface	Glyptal
Cold Surface	Glyptal
Full Flowrate	970 cc./min.
Barometer	746 mm. Hg.
Temperature	23.9°C.
Vacuum	2×10^{-5} mm. Hg.
Height at Start	15.5 cm.
Material of Sample Container	Monel
Flowmeter Used	Wet Test Meter

Flowrate

Time (min.)	Rate (cc./min.)
0	-
13	949
21.4	926
35	915
45	892
61	872
70.7	855
94.5	835
112.5	810
126.5	793
137.3	782
149.0	767
174.5	745
202.5	716
220.3	700

Description of Cold Surface

Glyptal was painted on monel and baked at 125°C. for 2 hours after air drying overnight. The resulting surface was clear, smooth, and uniform with a brownish tinge but transparent.

APPENDIX C

TABLE 7

Summary of Operating Data for Run 11

Hot Surface	Glyptal
Cold Surface	Scotch Tape
Full Flowrate	1237 cc./min.
Barometer	741.8 mm. Hg.
Temperature	24.2°C.
Vacuum	1×10^{-5} mm. Hg.
Height at Start	15.5 cm.
Material of Sample Container	Monel
Flowmeter Used	Wet Test Meter

Flowrate

Time (min.)	Rate (cc./min.)
0	-
5.6	1136
12.1	1121
24.8	1107
32.6	1085
39.6	1062
45.9	1048
51.4	1039
65.2	1014
70.7	1003
96.5	969
105.4	949
126.9	909
136.2	884
146.3	855
153.0	847

Description of Cold Surface

A layer of Scotch Tape was wrapped on a monel container. The tape was 2 cm. wide, clear, and transparent, but there were a few air bubbles in the surface.

APPENDIX C

TABLE 8

Summary of Operating Data for Run iii

Hot Surface	Glyptal
Cold Surface	Scotch Tape
Full Flowrate	1976 cc./min.
Barometer	743.6 mm. Hg.
Temperature	23.4°C.
Vacuum	9×10^{-6} mm. Hg.
Height at Start	15.3
Material of Sample Container	Monel
Flowmeter Used	Wet Test Meter

Flowrate

Time (min.)	Rate (cc./min.)
0	-
9.3	1883
13.8	1855
20.0	1824
27.9	1773
32.7	1750
39.2	1716
47.5	1668
57.8	1620
68.4	1575
77.6	1529

Description of Cold Surface

The cold surface is the same as Run ii but the outer hot surface has been changed to 2 coats of Glyptal.

APPENDIX C

TABLE 9

Summary of Operating Data for Run 1

Hot Surface	Lampblack
Cold Surface	Scotch Tape
Full Flowrate	2501 cc./min.
Barometer	745.7 mm. Hg.
Temperature	23.5°C.
Vacuum	1×10^{-5} mm. Hg.
Height at Start	15.2 cm.
Material of Sample Container	Monel
Flowmeter Used	Wet Test Meter

Flowrate

Time (min.)	Rate (cc./min.)
0	-
6.4	2362
10.0	2334
14.8	2283
21.1	2226
26.8	2155
34.1	2113
39.5	2065
45.1	2019
50.7	1971
58.0	1914

Description of Cold Surface

A layer of Scotch Tape was wrapped on a monel container. The tape was 2 cm. wide, clear, and transparent, but there were a few air bubbles in the surface.

APPENDIX C

TABLE 10

Summary of Operating Data for Run 2

Hot Surface	Lampblack
Cold Surface	Lampblack
Full Flowrate	2379 cc./min.
Barometer	743.5 mm. Hg.
Temperature	23.5°C.
Vacuum	2×10^{-5} mm. Hg.
Height at Start	15.3 cm.
Material of Sample Container	Monel
Flowmeter Used	Wet Test Meter

Flowrate

Time (min.)	Rate (cc./min.)
0	-
7.4	2314
11.2	2280
14.9	2260
19.9	2220
27.6	2138
33.0	2099
38.5	2056
45.4	1988
55.6	1912
67.8	1815

Description of Cold Surface

The lampblack-glyptal suspension after air drying overnight was baked at 125°C. for 1½ hours. This surface is the same as the hot surface. The surface was black and very rough.

APPENDIX C

TABLE 11

Summary of Operating Data for Run 3

Hot Surface	Lampblack
Cold Surface	Scotch Tape
Full Flowrate	2523 cc./min.
Barometer	746.1 mm. Hg.
Temperature	23.4°C.
Vacuum	1×10^{-5} mm. Hg.
Height at Start	15.3 cm.
Material of Sample Container	Monel
Flowmeter Used	Wet Test Meter

Flowrate

Time (min.)	Rate (cc./min.)
0	-
7.5	2351
12.3	2325
15.3	2294
22.2	2232
26.0	2215
35.4	2096
40.7	2056
47.7	1999
53.4	1948
63.8	1861

Description of Cold Surface

A layer of Scotch Tape was wrapped on a monel container. The tape was 2 cm. wide, clear, and transparent, but there were a few air bubbles in the surface.

APPENDIX C

TABLE 12

Summary of Operating Data for Run 4

Hot Surface	Lampblack
Cold Surface	Brass
Full Flowrate	304.0 cc./min.
Barometer	751.2 mm. Hg.
Temperature	24.5°C.
Vacuum	1×10^{-5} mm. Hg.
Height at Start	15.9 cm.
Material of Sample Container	Brass
Flowmeter Used	Capillary No. 3

Flowrate

Time (min.)	Rate (cc./min.)
0	-
10.5	219
25.7	330
29.7	306
38.8	292
41.9	348
46.7	304
51.8	285
54.4	281
56.3	281
60.9	278
64.0	278
68.7	275
72.6	275
83.2	272
103.6	267
109.6	266
120.2	261
134.9	257

Description of Cold Surface

The brass tubing was hand-polished with No. 92 Crocus Cloth made by the Carborundum Company. The resulting surface was bright and shiny with a few cuts.

APPENDIX C

TABLE 13

Summary of Operating Data for Run 5

Hot Surface	Lampblack
Cold Surface	Brass (tubing)
Full Flowrate	305.5 cc./min.
Barometer	753 mm. Hg.
Temperature	24°C.
Vacuum	1×10^{-5} mm. Hg.
Height at Start	15.7 cm.
Material of Sample Container	Brass
Flowmeter Used	Capillary No. 3

Flowrate

Time (min.)	Rate (cc./min.)
0	-
14	233
22.6	322
29.9	292
39.5	285
53.6	280
61	279
68.9	278.5
85.2	276.3
93.2	275
100	272.5
105.4	272
112.6	271
143.0	261
155	260
165	257.5

Description of Cold Surface

The brass tubing was hand-polished with No. 92 Crocus Cloth made by the Carborundum Company. The resulting surface was bright and shiny with a few cuts.

APPENDIX C

TABLE 14

Summary of Operating Data for Run 6

Hot Surface	Lampblack
Cold Surface	Monel
Full Flowrate	360.7 cc./min.
Barometer	740.4 mm. Hg.
Temperature	24.0°C.
Vacuum	1×10^{-5} mm. Hg.
Height at Start	15.1 cm.
Material of Sample Container	Monel
Flowmeter Used	Capillary No. 3

Flowrate

Time (min.)	Rate (cc./min.)
0	-
10.2	300
17.2	353
27.2	266.4
32.6	365
39.2	363
67.3	347
90.3	332
100.7	326
112.2	324.5
125.7	320
131.7	317
141.2	314
154.8	312
166.2	313
171.9	309.5
196.4	305

Description of Cold Surface

A monel container was hand-polished with No. 92 Crocus Cloth made by the Carborundum Company. The resulting surface was bright and shiny.

APPENDIX C

TABLE 15

Summary of Operating Data for Run 7

Hot Surface	Lampblack
Cold Surface	Monel
Full Flowrate	356.3 cc./min.
Barometer	734.4 mm. Hg.
Temperature	24.1°C.
Vacuum	1×10^{-5} mm. Hg.
Height at Start	15.3 cm.
Material of Sample Container	Monel
Flowmeter Used	Capillary No. 3

Flowrate

Time (min.)	Rate (cc./min.)
0	-
12.3	326
15.3	345
23.7	352.5
52.3	336.5
82.3	337.0
102.7	334.0
111.4	329.0
132.9	322.0
144.8	320.0
159.8	317.0
181.3	312.0
205.0	309.0
217.2	309.0
224.5	306.0
249.4	303.0
276.8	298.3

Description of Cold Surface

A monel container was hand-polished with No. 92 Crocus Cloth made by the Carborundum Company. The resulting surface was bright and shiny.

APPENDIX C

TABLE 16

Summary of Operating Data for Run 8

Hot Surface	Lampblack
Cold Surface	Adhesive
Full Flowrate	245 cc./min.
Barometer	737.4 mm. Hg.
Temperature	19.5°C.
Vacuum	2×10^{-5} mm. Hg.
Height at Start	15.1 cm.
Material of Sample Container	Monel
Flowmeter Used	Wet Test Meter

Flowrate

Time (min.)	Rate (cc./min.)
0	-
4.0	2317
7.7	2288
12.6	2257
17.7	2203
21.6	2178
25.5	2138
32.3	2067
36.4	2039
41.9	2002
49.1	1931
52.1	1886
59.7	1849
65.7	1807
68.9	1784
76.9	1722
81.9	1671

Description of Cold Surface

General Electric Adhesive No. 7031 was brushed on a monel container. After air drying overnight, the thick coat of adhesive was transparent and had a brownish tinge.

APPENDIX C

TABLE 17

Summary of Operating Data for Run 9

Hot Surface	Lampblack
Cold Surface	Aluminum Foil
Full Flowrate	137.5 cc./min.
Barometer	734.4 mm. Hg.
Temperature	24°C.
Vacuum	1×10^{-5} mm. Hg.
Height at Start	15.5 cm.
Material of Sample Container	Monel
Flowmeter Used	Capillary No. 3

Flowrate

Time (min.)	Rate (cc./min.)
0	-
7.8	87
17.5	118
33.9	146
46.4	140
57.3	137.5
70.0	135
87.1	130
100.5	127.3
145.2	119
180.9	116
206.4	113
236.3	109
266.0	104.5
294.0	104.5
331.0	104.5
372.0	100
414.0	99

Description of Cold Surface

Aluminum foil was loosely wrapped around surface of Run 8 (lampblack). The side exposed to the radiator had previously been polished by the manufacturer. This was a household grade of foil produced by the Reynold's Company.

APPENDIX C

TABLE 18

Summary of Operating Data for Run 10

Hot Surface	Lampblack
Cold Surface	Brass (tarnished)
Full Flowrate	355 cc./min.
Barometer	742.2 mm. Hg.
Temperature	24.1°C.
Vacuum	1×10^{-5} mm. Hg.
Height at Start	15.1 cm.
Material of Sample Container	Brass
Flowmeter Used	Capillary No. 3

Flowrate

Time (min.)	Rate (cc./min.)
0	-
23.8	330
38.0	319
44.8	306.5
66.3	310
74.9	305
85.1	302
94.6	300
104.9	300
115	296
125.5	294.5
165.7	281
195	265
209.5	263

Description of Cold Surface

Previous hand-polished brass was tarnished in an oxidizing flame until the surface became dull. The surface had a brownish tinge. The oxidation was not uniform.

APPENDIX C

TABLE 19

Summary of Operating Data for Run 11

Hot Surface	Lampblack
Cold Surface	Bakelite
Full Flowrate	2421 cc./min.
Barometer	748.8 mm. Hg.
Temperature	21.7°C.
Vacuum	1×10^{-5} mm. Hg.
Height at Start	15.2 cm.
Material of Sample Container	Brass
Flowmeter Used	Wet Test Meter

Flowrate

Time (min.)	Rate (cc./min.)
0	-
2.7	2314
5.1	2300
7.5	2288
11.3	2240
13.9	2217
20.3	2178
24.2	2138
30.9	2082
33.7	2056
36.4	2039
47.7	1943
53.6	1900
58.1	1866
65.8	1841
72.1	1756
78.7	1699
99.6	1529
115.0	1331

Description of Cold Surface

The bakelite was air dried overnight and then baked at 135°C. for 2 hours. The resulting surface was non-uniform, brownish-red, and transparent.

APPENDIX C

TABLE 20

Summary of Operating Data for Run 12

Hot Surface	Lampblack
Cold Surface	Lampblack
Full Flowrate	2365 cc./min.
Barometer	749.6 mm. Hg.
Temperature	20°C.
Vacuum	1×10^{-5} mm. Hg.
Height at Start	15.2 cm.
Material of Sample Container	Brass
Flowmeter Used	Wet Test Meter

Flowrate

Time (min.)	Rate (cc./min.)
0	-
2.8	2322
5.3	2356
7.7	2291
10.2	2271
15.2	2254
20.3	2155
23.0	2138
32.4	2056
42.2	1985
52.3	1909
59.8	1852
67.6	1787
77.2	1722
87.4	1617
96.3	1541
105.7	1450
113.5	1405

Description of Cold Surface

Surface is as same as in Run 2. This surface was not baked whereas the lampblack surface in Run 2 was baked.

APPENDIX C

TABLE 21

Summary of Operating Data for Run 13

Hot Surface	Lampblack
Cold Surface	Wood's Metal
Full Flowrate	484.5 cc./min.
Barometer	745.2 mm. Hg.
Temperature	24.1°C.
Vacuum	1×10^{-5} mm. Hg.
Height at Start	15.0 cm.
Material of Sample Container	Brass
Flowmeter Used	Capillary No. 3

Flowrate

Time (min.)	Rate (cc./min.)
0	-
13.5	410
16.3	447.5
19.3	457.5
23.8	459
30.7	458.4
38.2	458
45.3	450.6
52.0	445
58.5	445
75.6	440
87.0	436.5
96.8	434
108.8	428
128.4	421
136.9	419.5
146.0	416

Description of Cold Surface

A coat of Wood's metal was applied to a brass container with a gas-air torch. The resulting surface was silver in color with a dull appearance. The surface was rough and not uniform.

APPENDIX C

TABLE 22

Summary of Operating Data for Run 14

Hot Surface	Lampblack
Cold Surface	Chromium
Full Flowrate	266.5 cc./min.
Barometer	744.6 mm. Hg.
Temperature	23.9°C.
Vacuum	1×10^{-5} mm. Hg.
Height at Start	15.5 cm.
Material of Sample Container	Monel
Flowmeter Used	Capillary No. 3

Flowrate

Time (min.)	Rate (cc./min.)
0	-
22.9	228.5
34.9	232.3
41.0	253
52.3	250
62.6	244
76.0	239
85.9	235
99.6	233
114.2	231
126.6	227
137.4	224
155.8	220
167.8	218
181.0	216
190.6	214.5
207.2	212

Description of Cold Surface

Chromium was plated on a monel container. The resulting surface was bright, shiny, and uniform.

APPENDIX C

TABLE 23

Summary of Operating Data for Run 15

Hot Surface	Lampblack
Cold Surface	Chromium
Full Flowrate	265.8 cc./min.
Barometer	745.5 mm. Hg.
Temperature	24.2°C.
Vacuum	1×10^{-5} mm. Hg.
Height at Start	15.9 cm.
Material of Sample Container	Monel
Flowmeter Used	Capillary No. 3

Flowrate

Time (min.)	Rate (cc./min.)
0	-
11.5	170
26.1	268
41.1	262
53.6	245
63.4	242.2
75.3	238.5
84.3	238
94.5	234
104.6	231.5
114.9	229.5
127.6	225
135.6	224
144.8	222
155.6	220
160.0	219
172.3	215

Description of Cold Surface

Chromium plated on a monel container. The resulting surface was bright, shiny, and uniform.

APPENDIX C

TABLE 24

Summary of Operating Data for Run 16

Hot Surface	Lampblack
Cold Surface	Apiezon N
Full Flowrate	520.5 cc./min.
Barometer	738.4 mm. Hg.
Temperature	23.4°C.
Vacuum	1×10^{-5} mm. Hg.
Height at Start	15.8 cm.
Material of Sample Container	Monel
Flowmeter Used	Wet Test Meter

Flowrate

Time (min.)	Rate (cc./min.)
0	-
11.9	529.0
22.7	515.4
33.1	506.9
45.6	488.5
67.9	487.1
79.5	482.9
91.3	475.8
103.2	471.5
182.8	441.8
195.6	437.3
208.6	430.7
222.5	426.2

Description of Cold Surface

A thin film of Apiezon N was placed on the chromium plated surface of Run 15. The film of grease was very thin, uniform, and transparent. Apiezon N manufactured by Metropolitan-Vickers Electrical Company Ltd.

APPENDIX C

TABLE 25

Summary of Operating Data for Run 17

Hot Surface	Lampblack
Cold Surface	40 Sn/60 Pb Solder
Full Flowrate	149.5 cc./min.
Barometer	743.3 mm. Hg.
Temperature	24°C.
Vacuum	7×10^{-6} mm. Hg.
Height at Start	15.9 cm.
Material of Sample Container	Brass
Flowmeter	Capillary No. 3

Flowrate

Time (min.)	Rate (cc./min.)
0	-
20.9	119
30.8	132
43.3	146
66.9	140
85.3	141
101.7	140
134.4	140
181.4	135
207.0	134
212.6	133
219.0	132.8
248.1	130
312.5	127.3
449.5	119

Description of Cold Surface

A coat of 40 Sn/60 Pb solder was placed on brass with a gas-air torch. The resulting surface was silvery in color but not uniform. Solder manufactured by National Lead Company.

APPENDIX C

TABLE 26

Summary of Operating Data for Run 18

Hot Surface	Lampblack
Cold Surface	Scotch Tape
Full Flowrate	2498 cc./min.
Barometer	737.9 mm. Hg.
Temperature	22.9°C.
Vacuum	1×10^{-5} mm. Hg.
Height at Start	15.1 cm.
Material of Sample Container	Monel
Flowmeter	Wet Test Meter

Flowrate

Time (min.)	Rate (cc./min.)
0	-
6.3	2351
8.6	2331
13.5	2294
18.5	2244
24.8	2195
31.4	2113
34.0	2107
42.3	2036
52.2	1963
61.0	1880
68.7	1810
75.0	1733
79.9	1719

Description of Cold Surface

Triplicate of Run 1 and Run 3.

APPENDIX C

TABLE 27

Summary of Operating Data for Run 19

Hot Surface	Lampblack[10]
Cold Surface	Scotch Tape
Full Flowrate	605 cc./min.
Barometer	736.4 mm. Hg.
Temperature	23.4°C.
Vacuum	1×10^{-5} mm. Hg.
Height at Start	15.6 cm.
Material of Sample Container	Monel
Flowmeter Used	Wet Test Meter

Flowrate

Time (min.)	Rate (cc./min.)
0	-
8.4	616.0
24.0	582.2
32.3	574.4
44.1	566.0
58.0	556.5
62.8	553.0
70.5	544.0
76.1	545.0
80.7	542.2
107.0	522.0
112.0	520.0
126.0	511.0

Description of Cold Surface

Scotch Tape on monel tubing. Same surface as the previous Scotch Tape runs.

---

[10]Hot surface at 194.2°K.

APPENDIX D

CALIBRATION OF CAPILLARY FLOWMETER

The design of the system used for calibration of the capillary flowmeter with its three capillaries is shown in Figure 10. The scheme consist of: (1) a nitrogen source (A) which in this case is a compressed nitrogen cylinder, (2) a needle valve for flow control, (3) a saturation vessel (B) for saturating the dry nitrogen, and (4) a vessel (E) for the displacement of water by the saturated nitrogen gas.

The calibration of the capillaries was simple. The siphon (G) on the vessel (E), which is filled with water, is adjusted to give a desired reading on the flowmeter (D). At various times, the readings were taken from the water manometers (C) and (F) on both vessels, and from the capillary flowmeter. The displaced water from the siphon was collected in a volumetric flask at various known times. The volumetric flasks used had capacities of 100, 250, and 500 ml. depending on the diameter of the capillary being calibrated. An example of a plot of time versus the various readings taken is given in Figure 11. The curves obtained did not have zero slopes but have finite slopes which indicates a non-equilibrium calibration. This fact is due to the change in head of the water in the displacement vessel (E). To prove that there is no significant effect due to this

Figure 10

Calibration System for Capillary Flowmeter

A = Nitrogen Cylinder

B = Saturation Vessel (20 Liters)

C = Water Manometer

D = Capillary Flowmeter

E = Displacement Vessel (20 Liters)

F = Water Manometer

G = Siphon

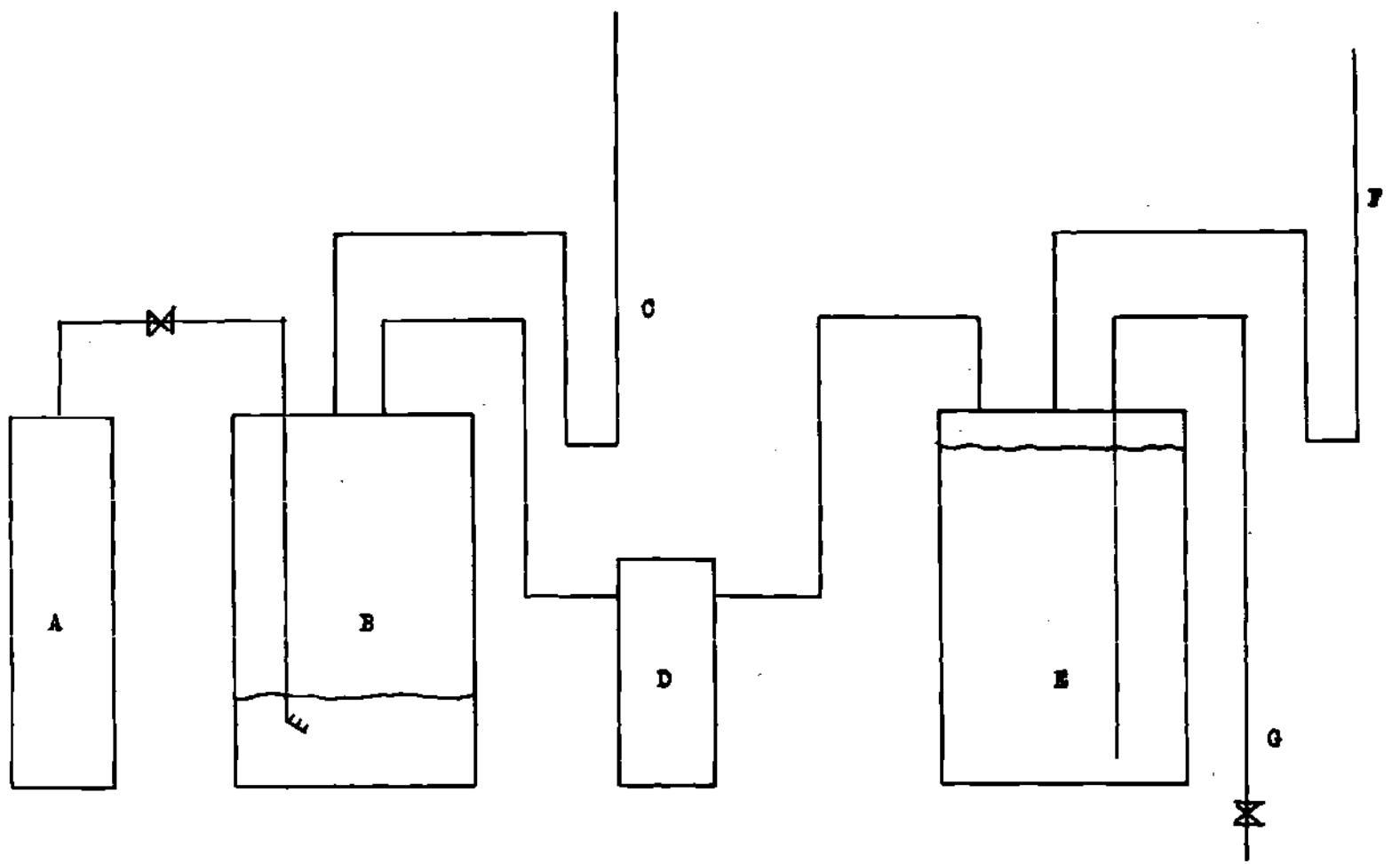
A
B
C
D
E
F
G

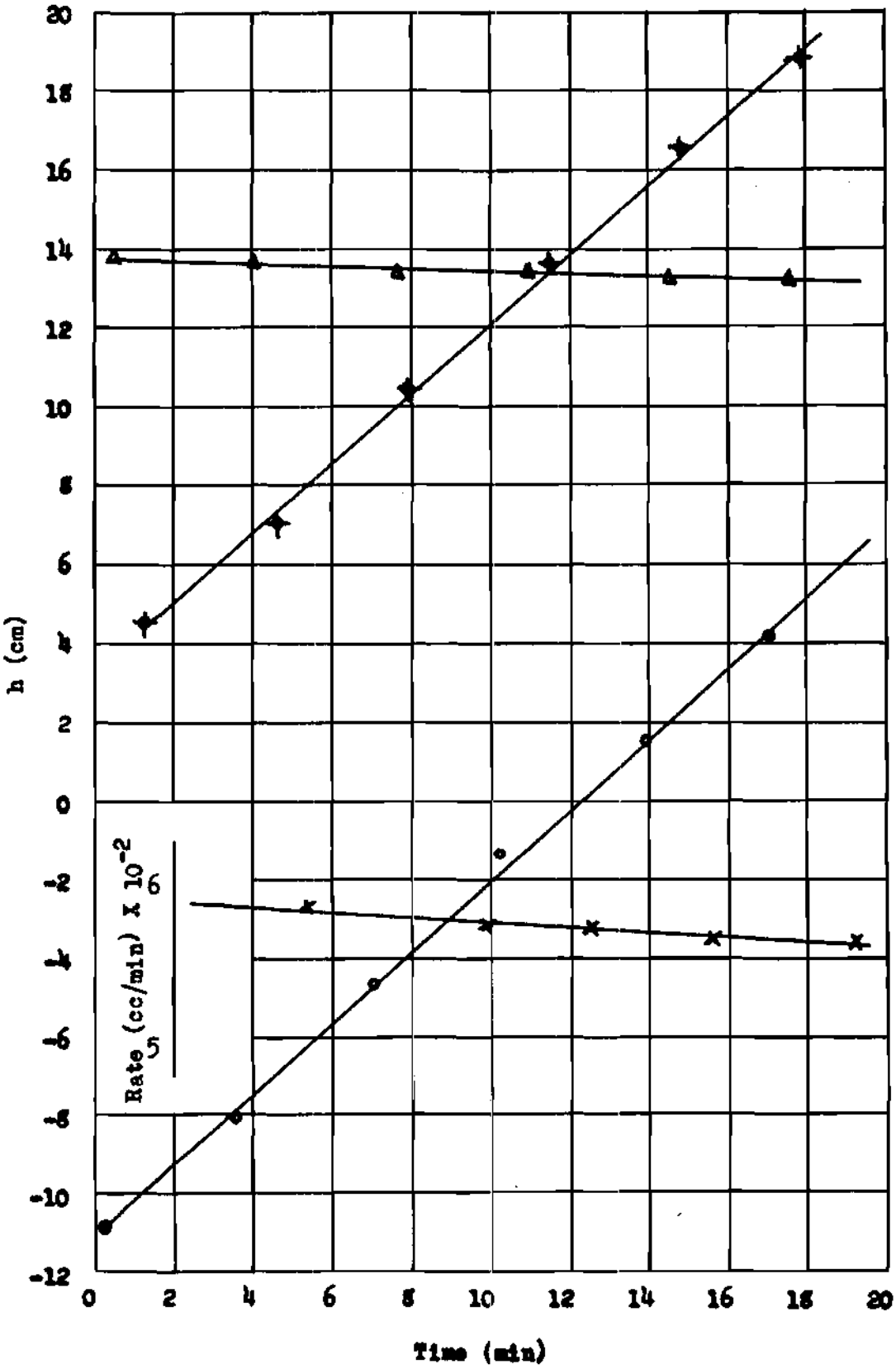
20
18
16
14
12
10
8
6
4
2
0
-2
-4
-6
-8
-10
-12
h (cm)
0
2
4
6
8
10
12
14
16
18
20
Time (min)
Rate (cc/min) x 10^{-2}
5
6

Figure 11

Various Readings Versus Time

△ = Capillary Flowmeter Reading

✦ = Water Manometer (C) Reading

○ = Water Manometer (F) Reading

× = Rate of Flow from Siphon

non-equilibrium, a calibration was made with better control of the needle valve, so that the system was very much nearer equilibrium.

In checking the flowmeter reading, the difference in the manometer readings should be equal to the pressure drop in the capillary since the slight pressure drop of the connections can be neglected. This fact can be illustrated from Figure 11. For a time of 10 minutes, water manometer (C) reads 12.1 cm. and water manometer (F) reads -2 cm., giving a pressure drop of 14.1 cm. of water. The capillary flowmeter reads 13.42 cm. of dibutyl phthalate, converting to centimeters of water gives 13.42 x 1.045 (see reference 30, page 136 for specific gravity of dibutyl phthalate) or 14.04 cm. of water which is a difference of approximately 0.4 per cent.

Since the theory of the flow of gases through a capillary tube is well known, only a brief discussion will be given with respect to the calibration and the actual use of the flowmeter. Facts to be considered are (1) the temperature varied in the neighborhood of 2 to 6 degrees centigrade during the calibration and varied as much as 10°C when used for a run, (2) the barometric pressure varied approximately 10 mm. of Hg., and (3) the flowmeter reading was never over 25 cm. of water. The conventional flow equation for flow of gases through a capillary tube is given by Poisseuille's law (reference 14, page 245)

$$V = \frac{\pi (p_1 - p_2) R^4}{8 \eta L}$$

where

V = Volume rate of flow

p_1 = Inlet pressure

p_2 = Outlet pressure

R = Radius of capillary

L = Length of capillary tube

η = Viscosity

Therefore, for a constant pressure difference, the volume rate of flow is a function of the viscosity. Since the viscosity is independent of the pressure (see reference 14, page 187) at moderate pressures, the only error in the volume rate of flow would be the error introduced by the change in temperature. The error therefore would be approximately 0.3 per cent/°C assuming that the viscosity of the saturated nitrogen varies proportionally with that of pure nitrogen gas (see reference 30, page 370, calculated from Equation 2).

For more precise measurements at high rates, the "coefficient of slip" should be considered. Also for short capillaries, end effects should be considered (see reference 14, page 246).

The calibration curves for the three capillaries are given in Figure 12. Table 28 is a summary of the calibration data.

Figure 12

Calibration Curves

1 = Capillary No. 1 (T = 27°C, P = 745 mm. Hg.)

2 = Capillary No. 2 (T = 30°C, P = 746 mm. Hg.)

3 = Capillary No. 3 (T = 30°C, P = 742 mm. Hg.)

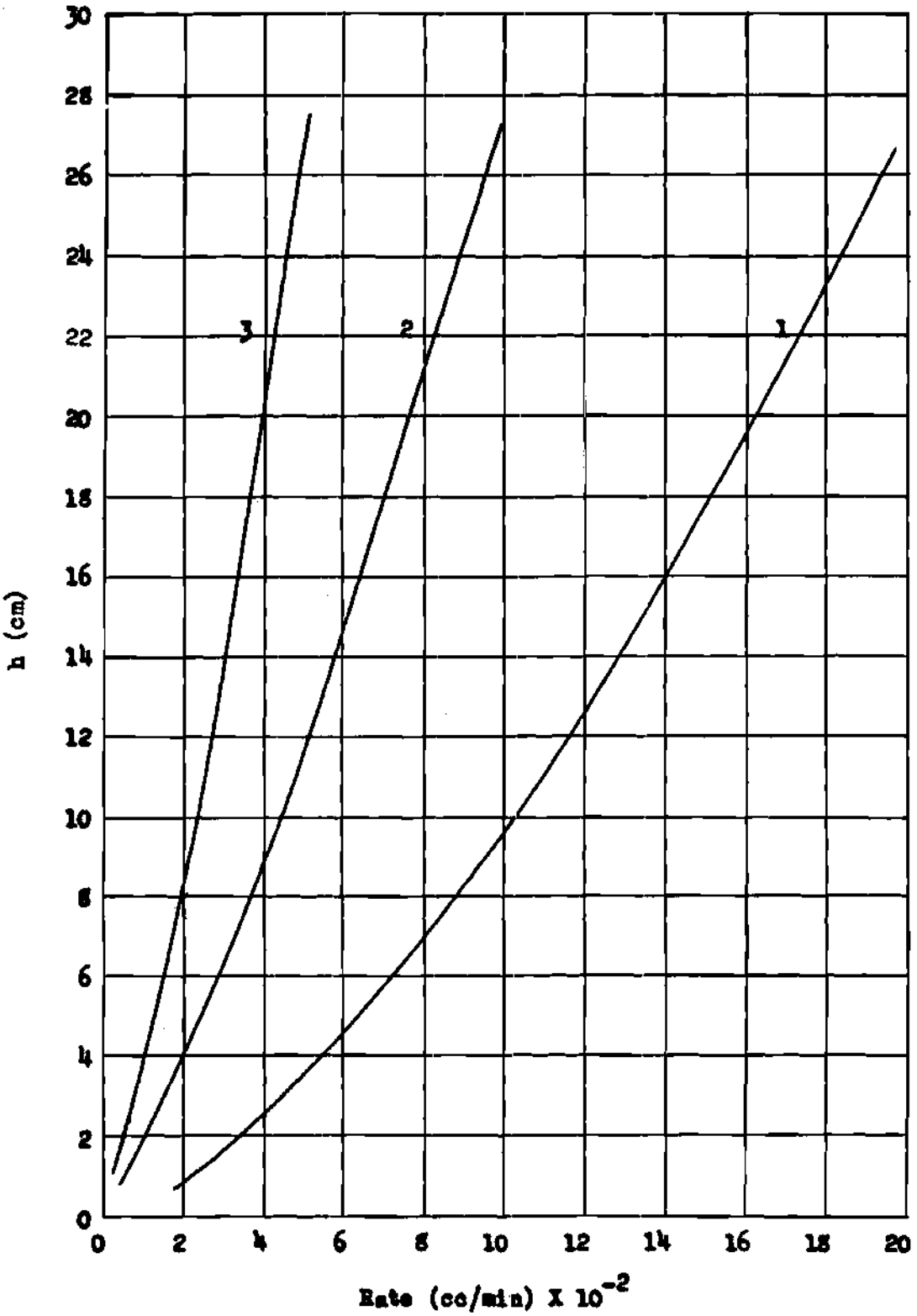
30
28
26
24
22
20
18
16
14
12
10
8
6
4
2
0
h (cm)
0
2
4
6
8
10
12
14
16
18
20
Rate (cc/min) X 10^{-2}
1
2
3

TABLE 28

Summary of Calibration Data for Capillary Flowmeter

Capillary No.	h (cm.)	Rate (cc./min.)	T (°C.)	P (mm. Hg.)
1	2.88	446	26.9	745
1	5.10	672	26.8	745
1	7.25	846	26.8	745
1	12.55	1210	27.0	745
1	14.50	1321	27.0	745
1	17.10	1452	27.0	745
1	21.34	1702	27.0	745
2	0.80	54	31	746
2	8.20	400	31	746
2	9.20	410	30	746
2	13.47	580	30	746
2	13.81	581	30	746
2	15.11	621	30	746
2	19.35	738	30	746
2	20.88	788	30	746
2	22.98	860	30	746
3	3.93	106	29.8	742
3	7.49	178	29.8	742
3	9.67	224	29.8	742
3	10.90	246	30.2	742
3	12.06	269	30.2	742
3	14.10	302	30.2	742
3	14.68	314	30.2	742
3	19.36	382	30.2	742
3	25.00	421	30.2	742

APPENDIX E

GASEOUS CONDUCTION ACROSS THE VACUUM SPACE

In order to estimate the energy transmitted by gaseous conduction, a modified form of the Knudsen equation was applied. The constant (N) for air was evaluated by Ryabinin (5). The equation

$$Q_g = N \sqrt{\frac{273}{T}} \ (T_2 - T_1) \cdot P \cdot S$$

has already been discussed in Chapter I. Inserting the condition imposed by the cryostat

$T_2 = 273^{\circ}K$

$T_1 = 77.4^{\circ}K$

$P = 1 \times 10^{-5}$ mm. Hg.

$S = 370$ cm^2 (inside surface)

$N = 0.317 \times 10^{-2}$ $\frac{\text{cal}}{\text{sec mm. Hg. cm}^2\ ^{\circ}K}$

$T = 175.2^{\circ}K$

Q_g becomes 0.172 cal./min.

APPENDIX F

CALCULATION OF X FACTOR

A sample calculation of the X factor will be given in this appendix. As an illustration Run 12 (lampblack-lampblack) will be used. The heat transmission for this run was 126.8 cal./min. for a full container and the emissivity was 0.866. Extrapolating the straight line portion of the time versus flowrate curve to zero height, the zero height flowrate corresponds to 65.2 cal./min. This extrapolation was accomplished in the same manner as the extrapolation for the full flowrate in Chapter III. Knowing the emissivity, the heat transmitted by the disk and the tube apertures can be evaluated by the last three terms of Equation (15). The heat transmitted by the disk and the tube apertures was found to be 10.4 cal./min. The heat transmitted to the cylindrical portion of the container is 126.8 cal./min. minus 10.4 cal./min. As the liquid level approaches zero height in the container, the evaporation rate is due to the heat transmitted to the bottom disk, to X times the heat transmitted to the cylindrical portion, and to the heat transmitted through the tube apertures. Therefore, X times the heat transmitted to the cylindrical portion must be 65.2 cal./min. minus 10.4 cal./min. Then

$$X = \frac{65.2 - 10.4}{126.8 - 10.4} = 0.47$$

In order to account for the temperature rise in the cylindrical section with respect to the total heat transmission, 126.8 cal./min., the following rough estimation was made:

(1) Since the operating data in Appendix C was obtained before the liquid level of the sample container decreased two inches, the estimation is for a liquid level drop of two inches.

(2) The cylindrical section of the above sample container (Appendix C, Run 12) was made from a $2\frac{1}{2}$ in. x 0.065 in. brass tube. The solid cross sectional area, therefore, is 0.5025 sq. in.

(3) The following assumptions are now made:

(a) the X factor is assumed to be approximately 0.5

(b) the molecular weight of brass is assumed to be 65 gm.

(c) it is assumed that the Debye Theory holds for brass and that

$$\theta_{Brass} = N_{Zn}\,\theta_{Zn} + N_{Cu}\,\theta_{Cu}$$

where θ = Debye θ, N_{Zn} = mole fraction zinc, N_{Cu} = mole fraction copper.

(4) The heat flux to the liquid nitrogen from the unfilled section is

$$q = (126.8 - 10.4)\ 2/6.625\ (0.5)$$

or 17.56 cal./min.

(5) From Fourier's law, ΔT is equal to 0.76°C., thermal conductivity of brass = 0.6 watts/cm.°C., Figure 27, reference 28, page 49.

(6) Knowing the density of brass, the heat capacity of brass (Figure 2, reference 30, page 298), and assuming a linear temperature distribution for the temperature difference, the energy utilized by the temperature rise is 1.4 cal./min.

APPENDIX G

ESTIMATION OF TEMPERATURE GRADIENT ACROSS RADIATING LAMPBLACK FILM

Since energy transmitted by radiation is a function of the fourth power of the absolute temperature, it is obvious that a significant temperature drop across the outer jacket of the cryostat described in Chapter III would produce a significant error in the calculations. An estimation of the temperature gradient across the wall and the film of lampblack of the outer jacket will be presented in this appendix. The thickness of the lampblack film was measured in an indirect way. A similar lampblack film was painted and baked under the same conditions as the original film upon a brass sheet. Measurements were made before and after application of the lampblack with a micrometer. The estimated thickness was 0.04 mm.

For heat transmission by conduction the familiar Fourier equation for steady state conduction was used.

$$Q_c = \frac{K A \Delta T}{L}$$

Where

K = thermal conductivity

A = cross-sectional area

L = length

ΔT = temperature gradient

Since the largest temperature gradient will be obtained with the largest heat transmission, the case of Scotch Tape will be used. The heat transmitted in this case is 130.4 cal./min. or 2.17 cal./sec. The thermal conductivity of brass at 273°K is 0.263 cal./sec. cm.°K (28). The thermal conductivity of the plastic was taken to be approximately equal to that of lucite which is 5×10^{-4} cal./sec. cm.°K (29). Therefore, the temperature gradient is

$$\Delta T_{brass} = \frac{(2.17)(0.165)}{(.263)(433)} = 0.0031^{\circ}C$$

$$\Delta T_{plastic} = \frac{(2.17)(0.004)}{(5 \times 10^{-4})(433)} = 0.0768^{\circ}C$$

The total temperature gradient is 0.08°C which is not significant since a one degree gradient will produce an error of approximately four per cent.

APPENDIX H

DISCUSSION OF EQUATIONS (15) AND (19) AND SAMPLE CALCULATIONS

(1) A supplementary discussion of Equation (19) will be presented in the first section of this appendix. With reference to Chapter III, page 45, Equation (19) is

$$Q = R_r \left(\frac{P_B}{P_o} \cdot \frac{T_o}{T} \cdot \frac{MW}{V_o} \cdot \frac{P_B - P_w}{P_B} \right) H_v \qquad (19)$$

The full flowrate (R_r) can be obtained from Appendix C. The term $(P_B - P_w)/P_B$ takes into account the fact that the nitrogen gas was saturated (nitrogen plus water vapor). The terms, P_B/P_o and T_o/T, reduces the volume rate of flow to that of standard conditions. The term MW/V_o converts volume rate of flow to mass rate of flow. The mass rate of flow times the heat of evaporation per gram (H_v) gives the heat transmitted.

(2) Sample calculations for a run involving the wet test meter and a run involving the capillary flowmeter are given in this section. Equation (20) in Chapter III is valid for both calculations. In the case of the capillary flowmeter, the full flowrate (R_r) has to be corrected by the term

$$\frac{P_B \cdot T_c}{P_{B_c} \quad T}$$

As an illustration for a run involving the wet test meter, consider Run 12 (Lampblack-Lampblack). Referring to Appendix C, page 81

$$R_r = 2365 \text{ cc./min.}$$
$$T = 293^{\circ}K$$
$$P_B = 749.6 \text{ mm. Hg.}$$
$$P_w = 17.5 \text{ mm. Hg.} \quad (30)$$

Equation (20) states that

$$Q = C\, R_r \, \frac{P_B - P_w}{T}$$

where C = constant = $0.002137 \frac{(\text{cal.})\ (^{\circ}K)}{(\text{cc.})\ (\text{mm. Hg.})}$

Substituting into Equation (20)

$$Q = 0.002137\ (2365)\ \frac{(749.6 - 17.5)}{295}$$

the heat transfer is 126.5 cal./min. Using Figure 3, e_2 equals 0.86.

As an illustration for a run involving the capillary flowmeter, the calculation for the emissivity of aluminum foil will be presented. Referring to Run 9 in Appendix C, page 78

R_r = 137.5 cc./min.

T = 297°K

P_B = 734.4 mm. Hg.

P_w = 22.4 mm. Hg. (30)

Capillary No. 3

For Capillary No. 3, T_c = 303°K and P_{B_c} = 742 mm. Hg., the correction therefore is

$$\frac{P_B\ T_c}{P_{B_c}\ T} = \frac{(734.4)\ (303)}{(742)\ (297^\circ K)} = 1.008$$

Substituting into Equation (20) as in the case of Lampblack-Lampblack

$$Q = (0.002137)\ (137.5)\ (1.008)\ \frac{(734.4 - 22.4)}{297}$$

the heat transfer is 7.05 cal./min. Again using Figure 3, e_2 equals 0.043.

(3) The general method of calculation for high emissivity surfaces was discussed in (2) with Lampblack-Lampblack surfaces as the illustration. The actual evaluation of the emissivity of the Lampblack-Lampblack surfaces was a trial and error solution of Equation (14) assuming e_1 equal to e_2. After obtaining a standard radiating surface, Equation (15) was derived for the cryostat and Figure 3 was constructed. Equation (15) is only valid for a radiating surface of lampblack, applied in the specific manner described in Appendix C, Runs 2 and 12.

APPENDIX I

CASE OF INFINITE PARALLEL PLANES VERSUS ACTUAL CASE

Since the radiating and receiving surfaces are reasonably close (0.185 inches between cylinders and 0.25 inches between disks, see Figure 2, page 19), it is expected that the actual case approaches the case of infinite parallel planes. The cases are represented by Equation (14) and (8), respectively. To compare the two cases, four calculations were made utilizing each equation, assuming e_1 equal to 0.866 and varying e_2. The results of these calculations are given in Table 29.

TABLE 29

Comparison of Equations (8) and (14)

e_2	Q cal./min. by Equation (8)	Q cal./min. by Equation (14)
1	141.51	143
0.5	75.91	76.55
0.1	16.17	16.2
0.05	8.15	8.21

Column 2 was calculated by means of Equation (8) with the assumption that the area (A_1) was equal to the inside area ($A_2' + A_4 = 361.5$ cm^2). The energy transmitted by the apertures of the tubes (0.11 cal./min.) was added to the above

calculation. The inside area was used rather than the outer area because of the fact that e_1 was approximately equal to one. Any F_{11} energy would be approximately absorbed.

BIBLIOGRAPHY

1. Dewar, J., Not. Proc. Roy. Inst. G. Brit., 14, 1-12 (1893).

2. Blackman, M., Egerton, A., and Truter, E. V., Proc. Roy. Soc. (London), A 194, 147-69 (1948).

3. Dewar, J., Proc. Roy. Soc. (London), A 71, 127 (1904).

4. The Report of the Oxygen Research Committee, H. M. S. O., London, 1923.

5. Ryabinin, Y. M., Avtogennoe Delo, No. 2, 19-21 (1946).

6. Banneitz, F., Rhein, G., and Kurge, B., Ann. Physik, 61, 113 (1920).

7. Briggs, H., Proc. Roy. Soc. Edinburgh, A 41, 97 (1920-1).

8. Hoag, L., Trans. Faraday Soc., 20, 327 (1924).

9. Meissner, W., Z. gas. Kalte - Ind., 37, 41-8 (1930).

10. Sydoriak, S. G., and Sommers, Jr., H. S., Rev. Sci. Instruments, 22, 915-919 (1951).

11. Henry, W. E., J. Applied Phys., 22, 1439 (1951).

12. Wexler, A., J. Applied Phys., 22, 1463-70 (1951).

13. Soddy, F. and Berry, A. J., Proc. Roy. Soc. (London), A 83, 254 (1910).

14. Loeb, L. B., Kinetic Theory of Gases, 1st ed. New York: McGraw-Hill Book Co. Ind., 1927, p. 270, 187, 246, 245.

15. Reynolds, M. M., Fulk, M. M., and Park, O. E., Proceedings Cryogenic Engineering Conference Sept. 8-10, 1954, Boulder, Colo., p. 151-157.

16. Roebuck, J. R., Rev. Sci. Instruments, 14, 90 (1943).

17. Griffiths, E. A., Trans. Faraday Soc., 18, 224 (1922).

18. Rips, S. M., Avtogennoe Delo, No. 1, 16-18 (1946).

19. Giauque, W. F., Rev. Sci. Instruments, 18, 852 (1947).

20. Henry, W. E., and Dolecek, R. L., Rev. Sci. Instruments, 21, 496-7 (1950).

21. Katan, L. L., Vacuum, 1, No. 3, 191 (1951).

22. Zimmerman, F. J., Ninth Calorimetry Conference, Schenectady, N. Y., Sept. 17-18, 1954.

23. McAdams, W. H., Heat Transmission, 3rd. ed. New York: McGraw-Hill Book Co., Inc., 1954, p. 58, 63, 65, 72.

24. Richtmyer, F. K. and Kennard, E. H., Introduction to Modern Physics, 4th ed. New York: McGraw-Hill Book Co., Inc., 1947, p. 166.

25. Langmuir, I., Adams, E. Q., and Meikle, G. S., Trans. Am. Electrochem. Soc., 24, 53-84 (1913).

26. Hamilton, S. C. and Morgan, W. R., National Advisory Committee for Aeronautics, Technical Note 2836, Washington, December, 1952, p. 25, 29, 32, 37, 66, 69.

27. Bloomer, O. T., and Rao, K. N., Thermodynamic Properties of Nitrogen, Institute of Gas Technology Research Bulletin 18 (October, 1952).

28. Powell, R. L. and Blanpied, W. A., Nat. Bur. Standards (U. S.), Circ. 556, 49 (1954).

29. Harris, F. K., Rev. Sci. Instruments, 14, 326 (1943).

30. Perry, J. H., Editor, Chemical Engineers' Handbook, 3rd ed. New York: McGraw-Hill Book Co., Inc., 1950, p. 149, 298, 370.